The Morphometric Properties of the Anterior Cruciate Ligament

by

Taylor McGee Price

B.S. Physics, West Virginia Wesleyan College, 2015

Submitted to the Graduate Faculty of

Swanson School of Engineering in partial fulfillment

of the requirements for the degree of

Master of Science

University of Pittsburgh

2020

UNIVERSITY OF PITTSBURGH

SWANSON SCHOOL OF ENGINEERING

This thesis was presented

by

Taylor McGee Price

It was defended on

March 12, 2020

and approved by

Mark C. Miller Ph.D., Associate Research Professor, Department of Mechanical Engineering and Materials Science

William Slaughter Ph.D., Associate Professor, Department of Mechanical Engineering and Materials Science

Patrick Smolinski Ph.D., Associate Professor, Department of Mechanical Engineering and Materials Science

The Morphometric Properties of the Anterior Cruciate Ligament

Taylor McGee Price, M.S.

University of Pittsburgh, 2020

The anatomy of the anterior cruciate ligament (ACL) has been thoroughly studied to further the understanding of functionality and pursue improvements in anatomical reconstruction [5]. Among the relevant studies are morphometrical investigations that analyze the cross-sectional area and shape of the ligament mid-substance and insertion sites [5][11][15]. The purpose of this study was to analyze additional geometric properties of the ACL along the mid-substance, including the first and second principal second moments of inertia, the major and minor axis lengths, and the major axis rotation relative to the anterior direction. Nine (n=9) fresh-frozen cadaveric knee specimens were tested. A six-degrees of freedom robotic testing system was used with a universal force-moment sensor to collect a passive path of flexion-extension, from full extension to 90°, by minimizing forces and moments about the intact knee joint for every 0.5° [5]. The femur and tibia were fixed in custom cylinders, with the femoral cylinder attached to a rigid base and the tibial cylinder fixed to the robot end-effector. The knee was carefully dissected until the tibial and femoral ACL insertion sites were exposed. Bone was then removed around the insertion sites to expose the ACL for laser scanning, and the cylinders were remounted on the robotic arm, maintaining the tibial-femoral position of the intact knee. A three-dimensional laser was used to scan the ACL at 15° of flexion and the tibial and femoral insertion sites were circumscribed using a 3 mm–diameter ball probe. A three-dimensional model of the ligament was used to calculate the cross-sectional properties. The angle of each cross-section was also varied in two directions in order to observe how the data changed. This

study confirmed previous descriptions of the ACL, such as having an hourglass structure [5], and having a “flat-ribbon” mid-substance [11]. It was found that the ratio of major-to-minor axis length decreased from the femoral insertion site to the tibial insertion site. The change in cross-sectional plane angles only showed a significant effect on the geometric data at 20° relative to the original angle.

Table of Contents

List of Tables

List of Figures

Preface

I would like to express my appreciation to my advisor, Dr. Patrick Smolinski, for his outstanding mentorship and research guidance throughout my graduate experience. I am also thankful for the constant direction and growth provided by Ms. Monica Linde within the Orthopaedic Engineering and Sports Medicine Laboratory. Special thanks to Michael DiNenna and Michael Smolinski for their assistance in this project, and others. I am also grateful for the assistance and partnership given by Dr. Tomomasa Nakamura. Having the opportunity to work with Dr. Carola Van Eck, Dr. Aly Fayed, and Dr. Yongtao Mao has been a true blessing for my personal and professional development. Brandon Marshall and Jun Jun Zhu were also pivotal in my early stages as a graduate student. Lastly, my gratitude is extended to my thesis committee members, Dr. Mark Miller and Dr. William Slaughter, and past professors.

1.0 Introduction

The anatomy of the anterior cruciate ligament (ACL) has been thoroughly studied to further the understanding of functionality and pursue improvements in anatomical reconstruction [5]. Among the relevant studies are morphometrical investigations that analyze the cross-sectional area (CSA) and shape of the ligament mid-substance and insertion sites [5][11][15]. Fujimaki et al. and Siebold et al. focused on the ACL mid-substance and the tibial insertion site, while Zheng and Harner et al. only measured the tibial insertion site. Each study applied different measurement techniques. Fujimaki used a three-dimensional (3D) laser scanner and averaged the area data for each specimen [5]. Zheng and Harner used CT-based measurements and averaged the tibial insertion outlines of the samples, then calculated the area of the average boundary [15]. Siebold used a macroscopic approach including calipers and digital photos, then averaged the results of all specimens [11]. The ACL mid-substance has been described as a flat, "ribbon"-like structure, along with a "C" shaped direct tibial insertion [11]. It has also been reported to have an "hourglass" shape with fan-like extensions at each insertion site [5]. The purpose of this study was to analyze the geometric properties of the native ACL cross-section along the mid-substance of the ligament, with no applied loads, using 3D laser technology. The geometric properties of nine (n=9) samples were analyzed, including CSA, first and second principal second moments of inertia, major and minor axis length, and major axis rotation relative to the anterior direction. Cross-sectional planes were also taken at varying orientations and compared to the original plane data. This study aimed to explore a mathematical method to more closely relate the ACL grafts used in anatomical reconstruction with the native ACL. A

better understanding of the ACL geometry may aid surgeons in graph size and shape determination, or graft harvesting techniques.

2.0 Background

Theoretical concepts and necessary terminology will be established to give an understanding of the methods used and data acquired in this study. A brief description of the anatomical directions will be presented, followed by some background information regarding the ACL and quantitative data analyzed in past studies. The relevant theory for each geometrical category in this study is outlined.

2.1 Anatomical Planes and Directions

A few anatomical terms must be covered to fully understand the information presented in this study (Figure 1). Considering the anatomical orientation of the human body, the sagittal plane separates the body into right and left segments and the coronal plane separates the body into front and back segments. Anterior and posterior are used to describe horizontal position in the sagittal plane, with anterior being towards the front of the body and posterior towards the back. The anterior-posterior direction is also considered the direction of the sagittal axis. Medial and lateral indicate horizontal directions in the coronal plane and are in the same direction of the coronal axis. Medial is closer to the midline of the body and lateral is closer to the outside. Proximal and distal are terms that relate limb position to the trunk, where proximal is closer to the trunk and distal is father away. Superior and inferior describe vertical position relative to the head and feet, where superior is closer to the head and inferior is closer to the feet. The superior-inferior direction corresponds to the axial or longitudinal direction of the body.

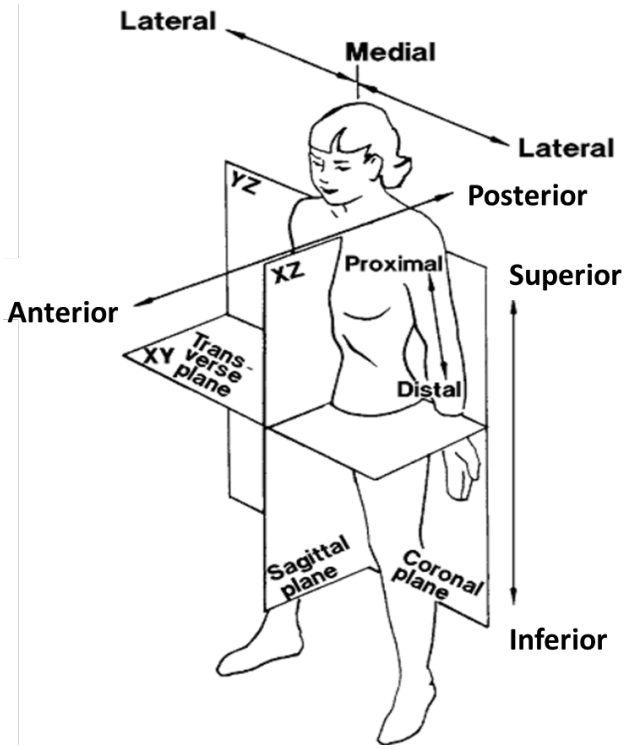

Figure 1 - Schematic of the anatomical planes and directions. [LarryFrolich.com]

2.2 Anatomy of the Knee

There are two articulations of the knee, patellofemoral and tibiofemoral. The patellofemoral articulation acts as an extensor of the tibia relative to the femur; the patella acts as a lever arm or hinge, while the quadriceps and patellar tendons transmit force generated by the quadriceps muscle to the tibia. The tibiofemoral articulation is comprised of capsular ligaments, tendons, cartilage, and menisci, along with muscles that span the joint, all of which play pivotal roles in the stability of the knee [2]. The main ligaments in the knee are the anterior cruciate ligament, posterior cruciate ligament, medial collateral ligament, and lateral collateral ligament. The ACL is foundational in restraining anterior tibial translation [10]. It also contributes to the

rotational stability of the tibia relative to the femur [6]. The ACL origin is located on the posterolateral surface of the intercondylar notch and the insertion is located anteriorly on the intercondylar eminence of the tibia [2] (Figure 2).

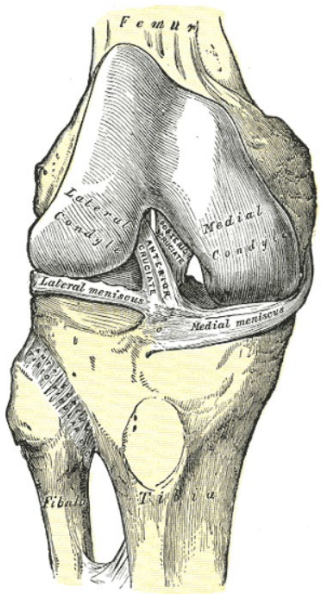

Figure 2 - Anterior view of the knee joint [Henry Gray (1825-1861). Anatomy of the Human Body. 1918.]

The ACL consists of two bundles, anteromedial and posterolateral, that spiral relative to each other [2]. The ACL is a "dynamic" structure, with each bundle experiencing various levels of tension through the flexion and extension of the knee [3][4]. It has been shown that not only does the ACL support rotary loads, but there is load sharing interaction between the bundles [6]. The CSA of the native ligament mid-substance and insertion sites play an important role in ACL reconstruction. A graft that is too small creates the risk for graft failure, but a large graft increases the chance for graft impingement [9]. Fujimaki et al. found that the average CSA of the tibial insertion was 175.8 ± 64.3 mm^2, where Zheng and Harner et al. reported a CSA of 114.9 ±

32.1 mm^2. Fujimaki et al. also concluded that the isthmus of the ligament when unloaded was located 49.4% of the distance from the tibial to the femoral insertion site and had an average CSA of 39.9 ± 13.7 mm^2. Siebold et al. reported the tibial insertion to have a CSA of 110.9 ± 14.7 mm^2. They also measured average cross-sectional dimensions of 9.9 mm and 3.9 mm with an average mid-substance CSA of 38.7 mm^2. Iriuchishima et al. and Hashemi et al. reported a mid-substance CSA of 46.9 ± 18.3 mm^2 and 52.6 ± 16.3 mm^2, respectively [7][8].

2.3 Geometric Measures

The geometric quantities of the ACL cross-section presented in this study are CSA, first and second principal second moment of inertia, major and minor axis length, and major axis angle relative to the anterior direction. The CSA is an important measure when determining anatomical reconstruction graft size and shape and studying the mechanical characteristics of the ligament. The principal moments of inertia are useful in describing the area distribution of a shape. They also determine the directions of the major and minor axes of an arbitrary shape. These directions can also be estimated by principal components analysis [12]. The relative major axis angle may give insight regarding how the major axis of the ACL cross-section changes direction along the length of the mid-substance, and the ratio of major-to-minor axis lengths can provide more information on how the shape changes along the ligament.

2.3.1 Cross-sectional Area

The CSA of an object is defined as the area of a two-dimensional (2D) surface that has been created by slicing a 3D object along one axis.

2.3.2 Second Moment of Inertia

The second moment of inertia is a 2D geometric property that describes how the area of a closed shape is distributed about an arbitrary axis. In mechanics, the second moment is related to the stress distribution in a linear-elastic material experiencing an applied bending moment. These are expressed in Cartesian coordinates by the following integrals:

$$I_{xx} = \int_A y^2 \, dA \tag{2.1}$$

$$I_{yy} = \int_A x^2 \, dA \tag{2.2}$$

$$I_{xy} = \int_A xy \, dA \tag{2.3}$$

where I_{xx} is the second moment about the x axis, I_{yy} is the second moment about the y axis, I_{xy} is the product of inertia, which is a measure of the symmetry of the shape, and dA is an element of area defined by x and y coordinates [14]. The second moments are dependent on the area of the cross-section and the orientation of the axes about which they are calculated. If the second

moment is known and the desired axes are rotated from an original orientation about a given origin, then the second moments about these axes are determined by a tensor transformation.

2.3.3 Parallel Axis Theorem

The parallel axis theorem states that the moment of inertia of an area with respect to any axis is equal to the moment of inertia around a parallel centroidal axis, plus the product of the area and the square of the distance between the two axes (Figure 3).

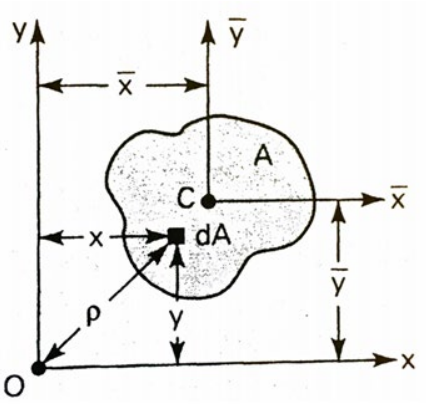

Figure 3 - Parallel Axis Theorem; relating the 2nd moment of a shape with respect to a centroidal axis to the 2nd moment with respect to an arbitrary parallel axis. [14]

Therefore,

$$I_{xx} = I_{\overline{xx}} + A\bar{y}^2 \tag{2.4}$$

$$I_{yy} = I_{\overline{yy}} + A\bar{x}^2 \tag{2.5}$$

$$I_{xy} = I_{\overline{xy}} + A\overline{x}\overline{y} \tag{2.6}$$

where $I_{\overline{xx}}$, $I_{\overline{yy}}$, and $I_{\overline{xy}}$ are the second moments and product of inertia with respect to the centroidal axis, A is the area, and $\bar{x}$ and $\bar{y}$ are the horizontal and vertical distances from the centroidal to the new axes [14].

2.3.4 Principal Second Moments of Inertia

Given any origin of interest, the principal second moments are the maximum and minimum second moments of an area about this origin. These values correspond to two perpendicular principal axis directions. The first principal axis is associated with the direction about which the areal distribution of a shape varies the most from the origin and the second principal axis defines the direction about which the areal distribution varies the least [14]. Typically, the principal second moments of an area are measured with the coordinate system origin located at the centroid of the shape. The relationship of principal second moments of inertia can be represented by the eigenvalue problem:

$$\underline{I}\underline{x} = \lambda\underline{x} \tag{2.7}$$

$$\underline{I} = \begin{bmatrix} I_{xx} & I_{xy} \\ I_{xy} & I_{yy} \end{bmatrix} \tag{2.8}$$

where I_{xx}, I_{yy}, and I_{xy} are the second moments and product of inertia with respect to a set of reference axes, λ is an eigenvalue of the system, and $\underline{x}$ are the eigenvectors.

The system of equations can be solved for the unknown variables λ_1, λ_2, $\underline{x}_1$ and $\underline{x}_2$. The eigenvalues of this system are the first and second principal moments of inertia and the eigenvectors of the system give the directions of the major and minor axes.

2.3.5 Principal Components Analysis

Principal Component Analysis (PCA) is a statistical procedure that highlights similarities and differences in a data set by reducing the dimensionality. PCA is beneficial in data sets of high dimensionality, where graphical representation is not possible [12]. For the purposes of this study, only the beginning steps of PCA were needed to compute major and minor axes. These results could then be compared to that obtained by the principal axes. The first step is calculating the means of each coordinate and subtracting them from the data set. Next is to calculate the variance of each dimension. The variance of a data set is a measure of the average distance of the data from the mean, given by

$$s^2 = var(X) = \frac{\sum_{i=1}^{n}(X_i - \bar{X})^2}{(n-1)}, \tag{2.9}$$

where s is the standard deviation, X_i is the i^{th} component of the X dimension, $\bar{X}$ is the mean of the X dimension, and n is the total number of points or observations. Then the covariance matrix can be assembled. In a set of data that is more than one dimension, the covariance is useful for finding relationships of how the dimensions vary from the mean with respect to one another [12]. The covariance is computed using two dimensions at a time. It is described by

$$cov(X,Y) = \frac{\sum_{i=1}^{n}(X_i - \bar{X})(Y_i - \bar{Y})}{(n-1)}. \tag{2.10}$$

Consequently, for a 3D set, six independent covariances can be determined. These values can be placed in matrix form with the diagonal elements representing the variances of the respective dimensions [12].

$$[C] = \begin{bmatrix} cov(X,X) & cov(X,Y) & cov(X,Z) \\ cov(Y,X) & cov(Y,Y) & cov(Y,Z) \\ cov(Z,X) & cov(Z,Y) & cov(Z,Z) \end{bmatrix} \tag{2.11}$$

The covariance matrix is symmetric and positive semidefinite, and the values of the terms in this matrix will change if the coordinate system is rotated. The most important property of a covariant is the sign, indicating a positive or negative relationship between dimensions. For instance, if the covariance of X and Y is positive, then as X increases farther from the mean, Y also increases farther from the mean. This would be indicated by a positive trendline. If the value is negative, then as X increases from the mean, Y decreases from the mean or conversely, Y increases while X decreases. If the value is zero, then the dimensions are independent of each other [12].

Lastly, the eigenvectors and eigenvalues of the covariance matrix can be determined. For a 2D covariance matrix, the orthogonal eigenvectors represent the coordinate system directions for which the diagonal terms are minimized and maximized and the off-diagonal terms are zero.

$$[C] = \begin{bmatrix} cov(X,X) & cov(X,Y) \\ cov(Y,X) & cov(Y,Y) \end{bmatrix} \tag{2.12}$$

These are called the principal components, the directional values for which a set of points is farthest from their mean and the other is closest to the mean. The eigenvalues of the system are the maximum and minimum variances, and the eigenvectors are the corresponding directions (Figure 4).

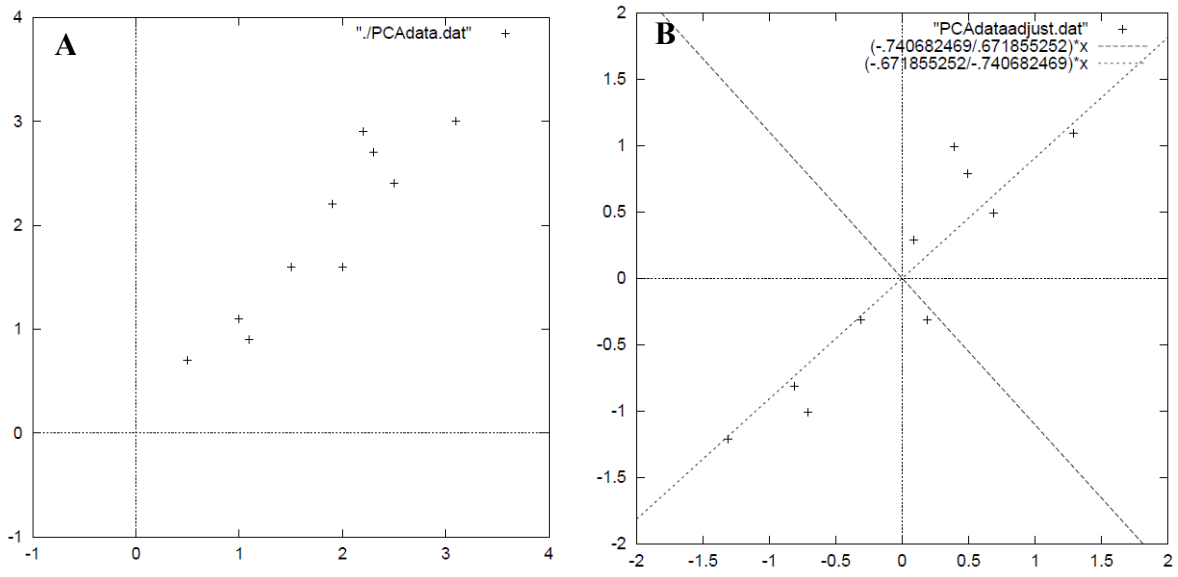

Figure 4 - Example 2D data set before mean adjustment (A) and with covariant eigenvectors (B) [12].

Graphically, for a 2D shape, with the coordinate origin at the centroid, the set of x and y coordinate points are spread the farthest from the means in the direction of the eigenvector that corresponds to the largest eigenvalue and are closest to the means in the direction corresponding to the other eigen value. For a closed shape, this indicates the directions where the boundary is distributed farthest and closest from the centroid. Consider an ellipse with equally spaced points along the boundary. Intuitively, the eigenvectors of the data points align with the major and minor axes. Notice that in the principal directions, there is no trend between the x and y

dimensions of the data points (Figure 5A). Also notice that when the points are projected onto each axis, the variance is the greatest in the x direction and least in the y direction (Figure 5B).

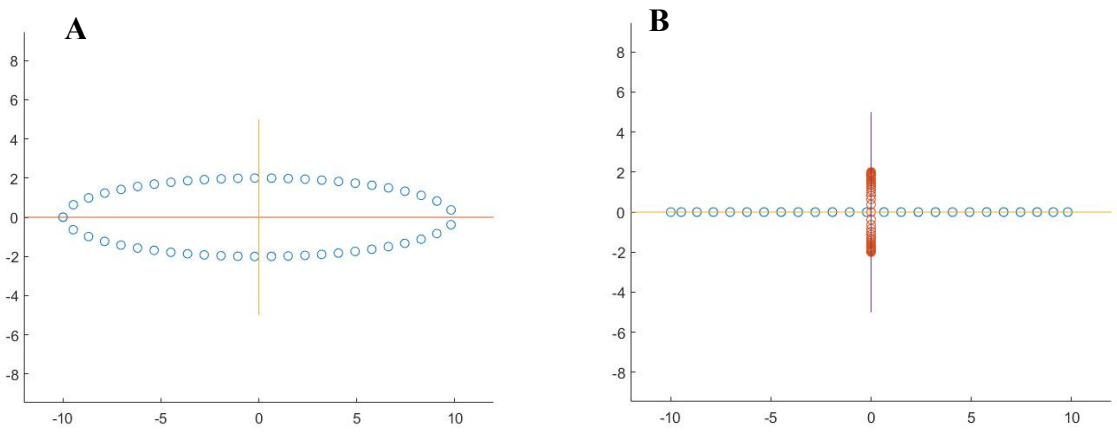

Figure 5 – Ellipse with equally spaced vertices (A) and the corresponding distribution of points along the eigenvectors (B).

Therefore the boundary of the ellipse is distributed closest from the center along the y axis and farthest from the center along the x axis. The major and minor axis lengths are related by a quadratic to the variances of the boundary and linearly to the standard deviation of the boundary. Generally, the higher the variances (eigenvalues), the longer the axis lengths.

Major and minor axis results using PCA are expected to be similar to those obtained by calculating the principal second moment axes. Both the second moment and variance calculations involve a summation that adds the squared distances of all of the elements of area around the cross-section from the centroidal axes times the areas of each element. Essentially, calculating the variance of the points around a boundary is analogous to calculating the second moment of the boundary, opposed to the entire area. This value is then divided by the sum of the

element areas around the boundary, which is equal to the length of the perimeter. Therefore, the major and minor axis directions of each calculation should not prove to be significantly different.

3.0 Methods

3.1 Specimen Preparation and System Set-up

Nine (n=9) fresh-frozen cadaveric knee specimens were tested with institutional approval. A six-degree of freedom robotic testing system was used with a universal force-moment sensor to collect a passive path of flexion-extension, from full extension to 90°, by minimizing forces and moments about the intact knee joint for every 0.5° [5]. The universal force-moment sensor was attached to the robot end-effector to sense knee reaction forces. The femur and tibia were potted in epoxy and fixed in custom cylinders after the epoxy hardened. The femoral cylinder was fixed to a rigid base and the tibial cylinder was fixed to the robot end-effector for manipulation (Figure 6).

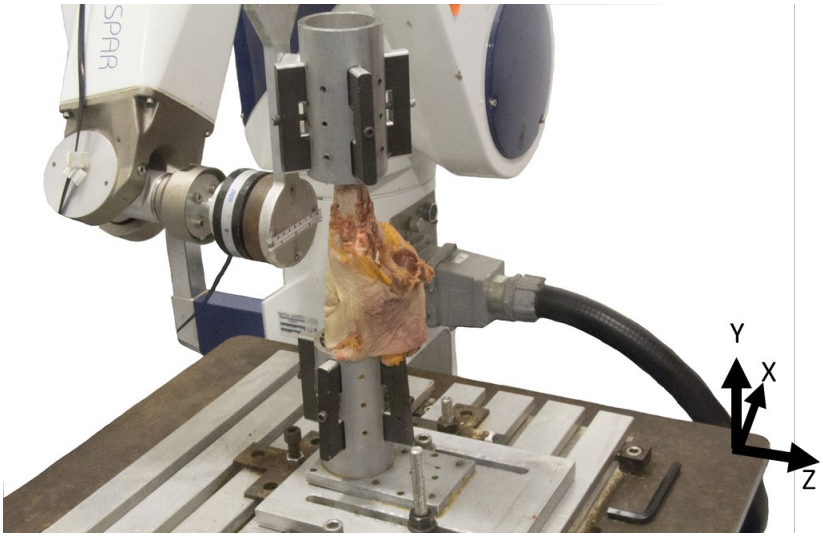

Figure 6 – Set up of robotic system, with the femur rigidly fixed and the tibia attached to the robot end-effector.

After capturing the intact knee flexion-extension path, the knee, remaining fixed in the cylinders, was carefully dissected until the tibial and femoral ACL insertion sites were exposed and the superficial synovium on the ACL mid-substance was removed. The degenerated fat tissues were identified and removed as well. Special care was taken throughout the dissection process to ensure that the superficial membrane of the ACL was unaffected. Bone was then removed around the femoral and tibial ACL insertion sites to expose the ACL for laser scanning (Figure 7), and the cylinders were mounted on the robotic arm, maintaining the tibial-femoral position of the intact knee. The intact passive path was then be replayed to recreate the ACL position during passive flexion-extension.

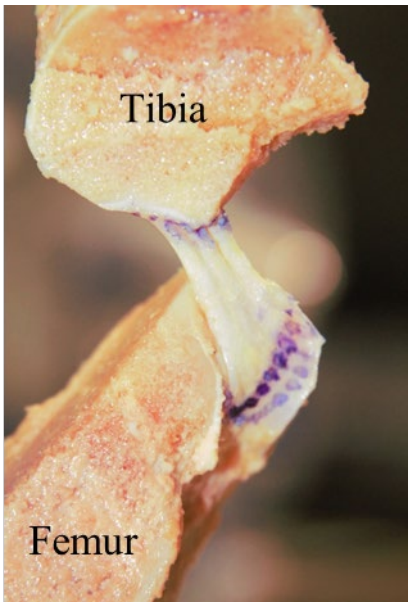

Figure 7 – Knee specimen after dissection process.

3.2 FaroArm Scanning and Probing

A 3D laser (FaroArm Platinum; Faro Technologies, Inc.) was used to scan the ACL at 15° of flexion and the tibial and femoral insertion sites were circumscribed using a 3 mm–diameter ball probe on the Faro coordinate measurement machine. Roughly 20-30 points were defined around each insertion site [5].

All scans and points were measured relative to a global coordinate system defined at the corner of the system table. The y-axis was defined normal to the top face of the table, which corresponded to the axial direction of the knee. The x and z directions were normal to the side faces of the table and completed a right-handed orthogonal system. Positive x corresponded to either the medial or lateral side of the knee, depending on whether the knee was left or right, and positive z corresponded to the posterior direction of the knee. The centroids of the 3D probe points were calculated using Microsoft Excel with the following equations:

$$x_{centroid} = \frac{1}{n}\sum_{i=1}^{n} x_i \tag{3.1}$$

$$y_{centroid} = \frac{1}{n}\sum_{i=1}^{n} y_i \tag{3.2}$$

$$z_{centroid} = \frac{1}{n}\sum_{i=1}^{n} z_i \tag{3.3}$$

A 3D model of the ACL was simultaneously assembled during scanning with Geomagic Inc. software based on the set of laser scan data (Figure 8).

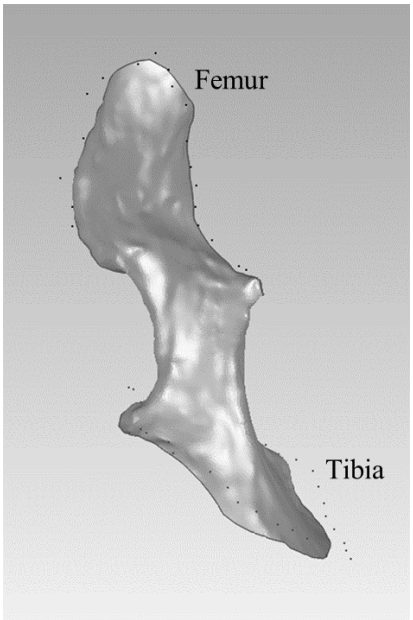

Figure 8 - 3D model of the ACL

The anatomical ACL axis was defined as the line connecting the femoral and tibial insertion site centroids, which were the average values of the probed points [5] (Figure 9). The normalized direction of this axis was calculated for future use. Using the probed points as a reference, user-defined insertion outlines were created on the ligament model to provide a visual representation of each insertion site (Figure 9). This was achieved by choosing points on the model surface to which Geomagic could then fit a spline.

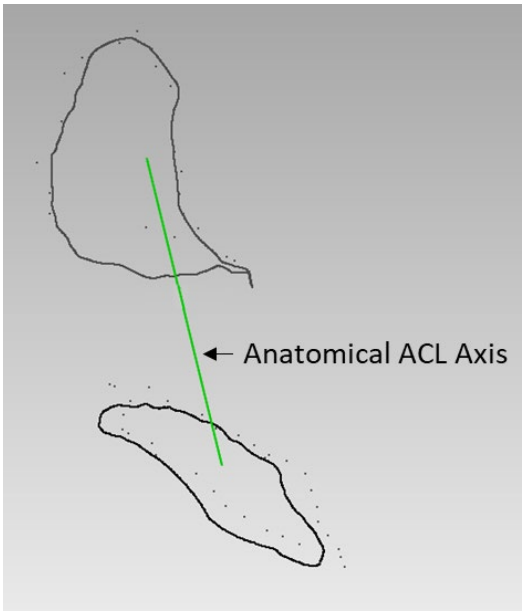

Figure 9 - Anatomical axis of the ACL determined by the line connecting the insertion site centroids. Pictured are the 3D probed points and the projected spline onto the ligament model.

3.3 Measurement of Cross-sectional Properties

To measure the ACL cross-sectional properties along the ligament, five planes were defined perpendicular to the ACL axis, equally spaced between the insertion sites of the ligament (Figure 10). The location of the top plane (Plane1) was selected to be as proximal as possible without intersecting the femoral insertion site, and the location of the bottom plane (Plane 5) was determined to be as distal as possible without intersecting the tibial insertion site. This ensured that there was no intersection of bone with the transverse planes closest to the ligament insertions sites.

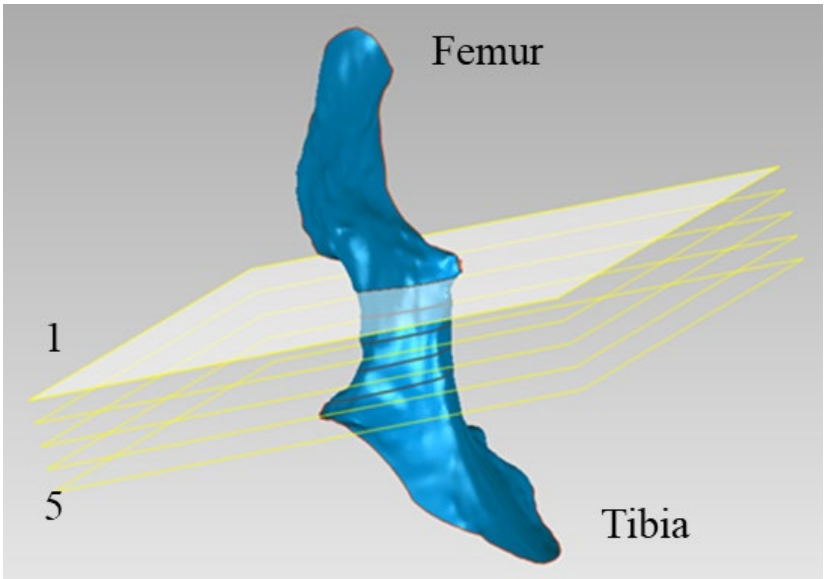

Figure 10 - 3D model of the ACL with cross-sectional planes.

Five cross-sectional outlines were defined by the points of intersection between the planes and the ligament model. Each outline was converted into one thousand equidistant points through a Geomagic function and exported to Excel. The cross-sectional points and ligament axis direction were then imported into MATLAB for data processing. Since the cross-sections are two-dimensional, it was necessary to convert the points (given by three-dimensions) around each cross-section into the 2D plane that was perpendicular to the ACL axis. To achieve this, a new coordinate system (primed) was established relative to the global system described in Section 3.2. with positive y in the direction of the femur, x being in the medial/lateral direction, and z in the anterior/posterior direction (axes used with the laser scanner). The $\boldsymbol{y'}$ axis components were defined as the normalized directions of the ACL axis vector. $\boldsymbol{x'}$ was determined to be an orthogonal vector to $\boldsymbol{y'}$. This was accomplished by interchanging the $\boldsymbol{x}$ and $\boldsymbol{y}$ components of $\boldsymbol{y'}$, multiplying the $\boldsymbol{y}$ component by -1, and setting the $\boldsymbol{z}$ component to 0. Each geometric quantity

was independent of the rotation of x' about y', therefore the only important condition in establishing x' was its orthogonality to y'. The z' axis was created by calculating the cross product of the $+x'$ and $+y'$ axes (Figure 11).

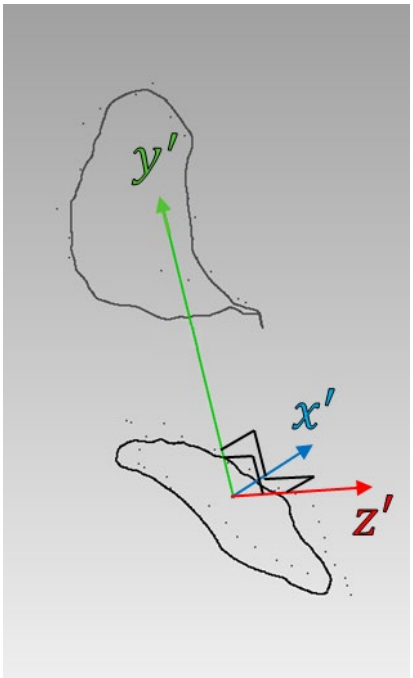

Figure 11 – Establishment of the transfomed coordinate system.

A matrix of cosines was used to transform the global coordinates of the system into local coordinates relative to the ACL axis, given by

$$[T] = \begin{bmatrix} cos\theta_{xx'} & cos\theta_{xy'} & cos\theta_{xz'} \\ cos\theta_{yx'} & cos\theta_{yy'} & cos\theta_{yz'} \\ cos\theta_{zx'} & cos\theta_{zy'} & cos\theta_{zz'} \end{bmatrix}, \quad (3.4)$$

where $cos\theta_{xx'}$ is the cosine of the angle between the original (x) and the transformed (x') axis.

The 3D cross-section points were calculated in terms of the transformed system by multiplying the transpose of the transformation matrix by the vector of each individual point:

$$[u]' = [T]^T[u], \tag{3.5}$$

where $[u]$ is the 3x1 vector of one boundary point with respect to the original coordinate system and $[u]'$ is the 3x1 vector of one boundary point with respect to the transformed coordinate system. After transforming each point along the boundary, this resulted in a constant y' value for every point along the cross-section, which indicated a successful transformation into the x'- z' plane (Figure 12).

Geomagic arranges points in descending order based on the x coordinate. To evaluate the geometric properties of the cross-sections, each point must be ordered based on consecutive position around the boundary in 2D space. The points were ordered in MATLAB by selecting one arbitrary point as the reference point, calculating the distance relative to each point along the curve, and placing the point with the smallest relative distance in the succeeding position. The next point became the reference point and the original point was excluded from the selection pool. This process was repeated until every point was accounted for and ordered properly (Figure 12).

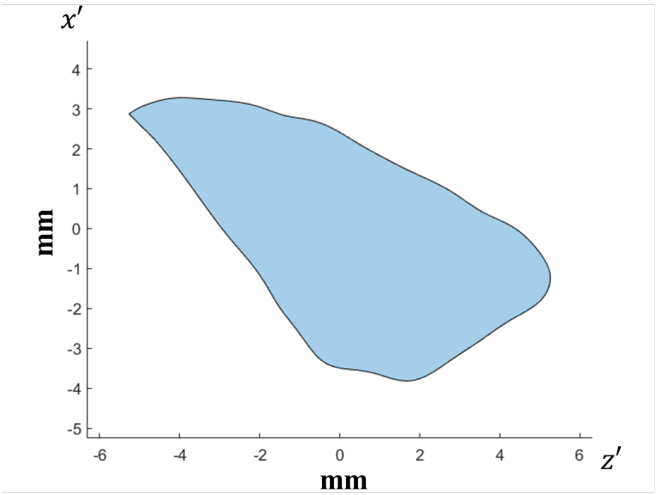

Figure 12 – Example cross-section of the ACL in the x'- z' plane.

3.4 Geometric Analysis

The geometric properties of the cross-sectional shape were analyzed. This included the cross-sectional area, first and second principal second moments of inertia, major and minor axis length, and major axis angle relative to the anterior direction. Each category was calculated using general equations that are dependent on the discrete points around a boundary. These equations will be discussed in the following sections. The major and minor axis lengths correspond to the centroidal second and first principal moment axes, respectively, where the centroidal axes pass through the centroid of the cross-section. The relative orientation of the major axis is with respect to the anterior direction projected onto the cross-sectional plane. PCA was also performed to compare the difference in major and minor axis data between that which was obtained by finding the centroidal second moments.

The centroid of each cross-section was calculated using the following equations:

$$x'_{centroid} = \frac{1}{n}\sum_{i=1}^{n} x'_i \tag{3.6}$$

$$z'_{centroid} = \frac{1}{n}\sum_{i=1}^{n} z'_i \tag{3.7}$$

The anterior and medial directions were projected onto each cross-sectional plot to help visualize the orientation of the cross-sections with respect to the anatomical directions of the knee. This was accomplished by defining points that resided on the x and z axes and transforming them onto the x'-z' plane. The line connecting the centroid and the transformed points indicates the anterior and medial/lateral directions (Figure 13).

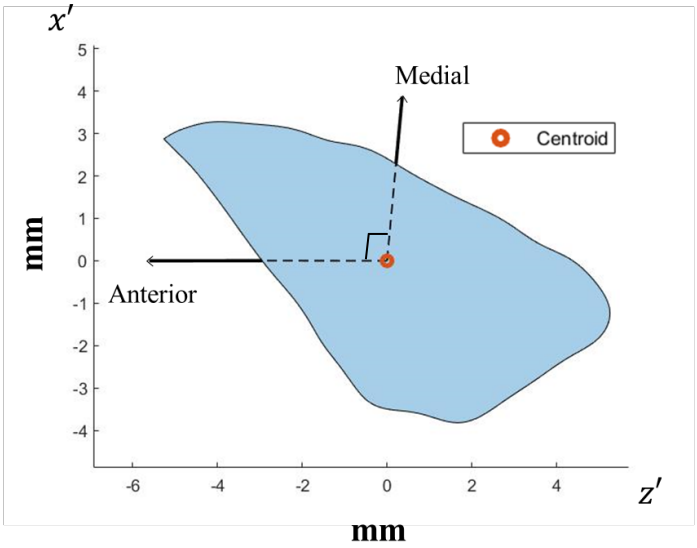

Figure 13 – Cross-sectional plot centered at the centroid with the anatomical directions labelled.

3.4.1 Area Calculations

The area inside a simple closed curve is given by, $\frac{1}{2}\oint x\,dy - y\,dx$. The integral can only be carried out if the equations of the curve are available. Since the outline of the ligament cross-sections in this study were converted into a series of points, the CSA's were calculated using Gauss' Area Formula, also known as the Surveyor's Formula. The surveyor's formula expresses the area of a polygon in terms of its vertices, which are the points at which two edges of the polygon meet. The area is given by,

$$A = \frac{1}{2}\sum_{i=1}^{n}\begin{vmatrix} x_i & x_{i+1} \\ y_i & y_{i+1} \end{vmatrix} = \frac{1}{2}\sum_{i=1}^{n}(x_i y_{i+1} - y_i x_{i+1}), \tag{3.8}$$

where x and y are the Cartesian coordinates of the vertices and n is the total number of vertices [1]. It is important that the first and last vertices are the same point.

3.4.2 Principal 2nd Moment Calculations

Similar to the CSA calculation, the principal second moments were calculated based on the set of equidistant points around the cross-section [7]. The equations for calculating the second moments of an area provided a set of vertices can be written as:

$$I_{xx} = \frac{1}{12}\sum_{i=1}^{n}(x_i y_{i+1} - x_{i+1} y_i)\,(x_{i+1}^2 + x_{i+1}x_i + x_i^2) \tag{3.9}$$

$$I_{yy} = \frac{1}{12}\sum_{i=1}^{n}(x_i y_{i+1} - x_{i+1} y_i)\,(y_{i+1}^2 + y_{i+1}y_i + y_i^2) \tag{3.10}$$

$$I_{xy} = \frac{1}{24}\sum_{i=1}^{n}(x_i y_{i+1} - x_{i+1}y_i)\,(2x_{i+1}y_{i+1} + x_{i+1}y_i + x_i y_{i+1} + 2x_i y_i) \qquad (3.11)$$

Once the second moment values were determined, the parallel axis theorem was used to calculate the second moments about the parallel axes that passed through the centroid. Next was to find the principal second moments and their respective axes by constructing the 2x2 matrix of second moments, where I_{xx} and I_{yy} are the diagonal components and I_{xy} is both the upper and lower components. The eigenvalues of this matrix corresponded to the first and second principal moments. The eigenvectors corresponded to the first and second principal axes.

3.4.3 Major and Minor Axis Lengths

The major and minor axis data were determined using two methods: finding the principal moment axes, and PCA. The major and minor axes derived from the principal moments corresponded to the eigenvectors of the second moment matrix. They corresponded to the eigenvectors of the covariance matrix when using the PCA method. The axis lengths were determined to be the distance between the two points of intersection between the axes and the border of the ACL cross-section:

$$l = \sqrt{(x_2 - x_1)^2 + (z_2 - z_1)^2}, \qquad (3.12)$$

where 1 and 2 are the points of intersection (Figure 14). The points of intersection were calculated by finding the points along the boundary that corresponded to the major and minor axis angles, relative to the centroid of the cross-section.

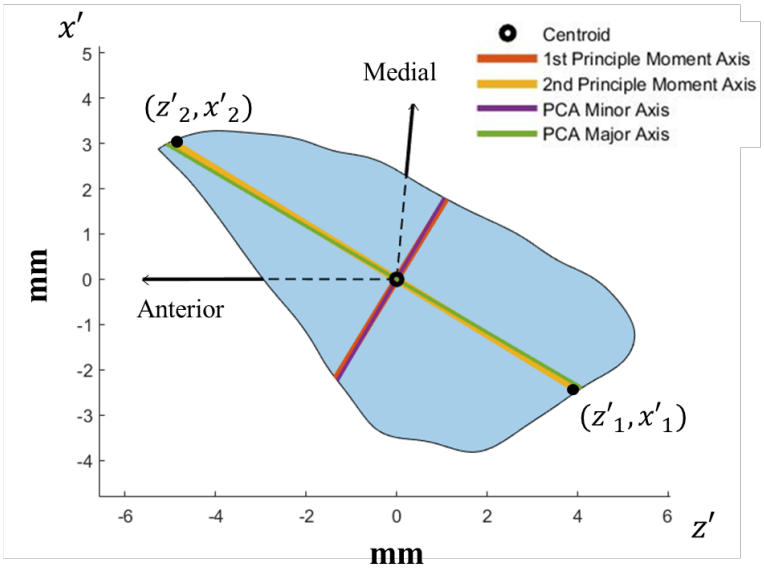

Figure 14 – Major and minor axes determined by the 2nd moment and PCA methods.

3.4.4 Major Axis Angle

The angle between the major axis and the anterior direction was calculated using

$$tan^{-1}\left(\frac{Y}{X}\right), \tag{3.13}$$

where X and Y are the normalized components of the minor axis vector.

3.5 Effect of Axis Variation

The ACL axis, the direction in which the perpendicular ligament cross-sections are analyzed, has been determined using different techniques [5][8][9][11]. This measure will vary depending on the method used. To assess the effect of changes in the cross-sectional orientation on the geometric properties, the ACL axis was varied in two perpendicular directions from 0°-20° in 5° increments. The first angle change was within the YZ (Axial-Anterior/Posterior) plane (Figure 15).

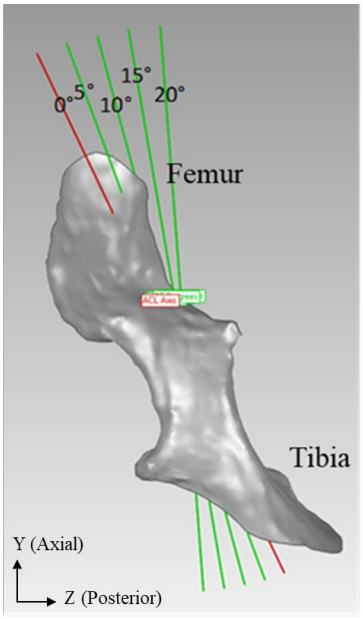

Figure 15 - ACL model with original axis (Red) and transformed axes (Green) in the YZ plane.

Each transformation was established uniformly within the YZ plane by holding the X (Medial/Lateral) coordinates of the original ACL axis constant. The same transformations were achieved in the XY (Medial/Lateral-Axial) plane by holding the Z coordinates constant (Figure 16).

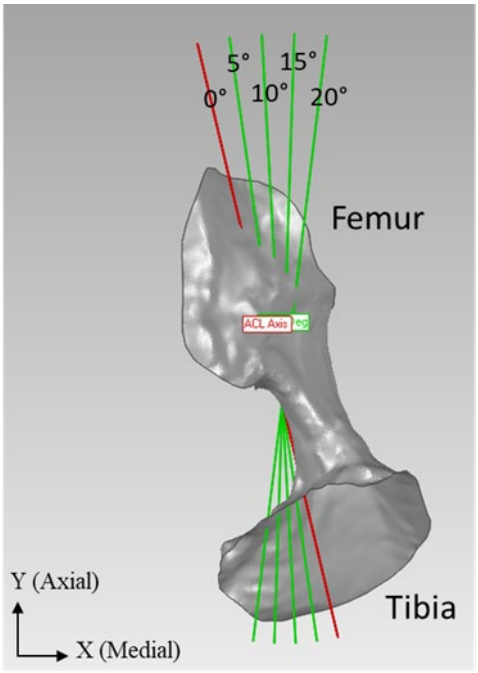

Figure 16 - ACL model with original axis (Red) and transformed axes (Green) in the XY plane.

One specimen was omitted from the XY transformations due to the inability to define a plane closest to one insertion without intersecting the other insertion. Therefore, in the XY direction, results are based on eight specimens. In all other knees, five additional parallel and equally spaced planes were defined, where the top plane was as proximal as possible without intersecting the femoral insertion site and the bottom plane was as distal as possible without intersecting the tibial insertion site. Figure 17 through Figure 20 display the variation of cross-sectional planes and curve position as the ACL axis is transformed in each direction.

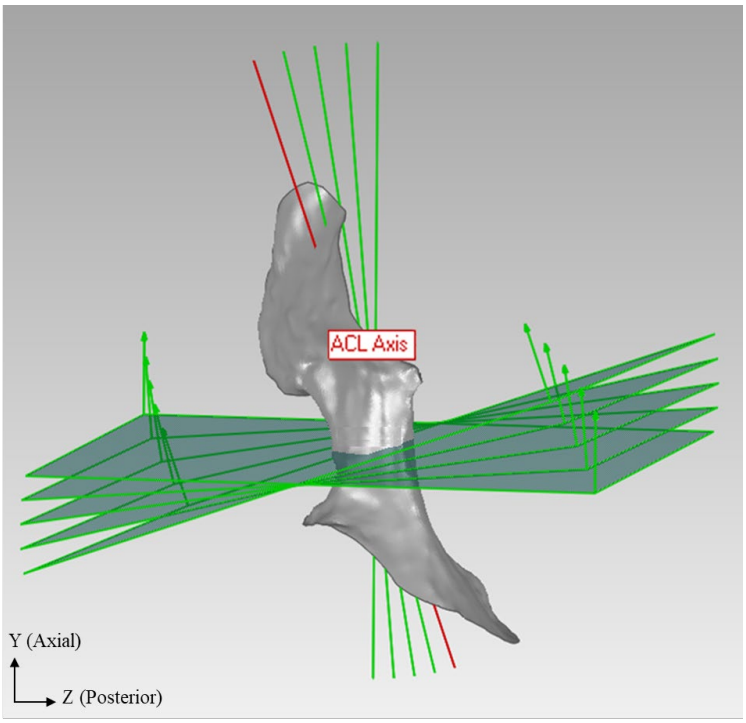

Figure 17 – Variation of planes at the middle cross-section in the YZ plane.

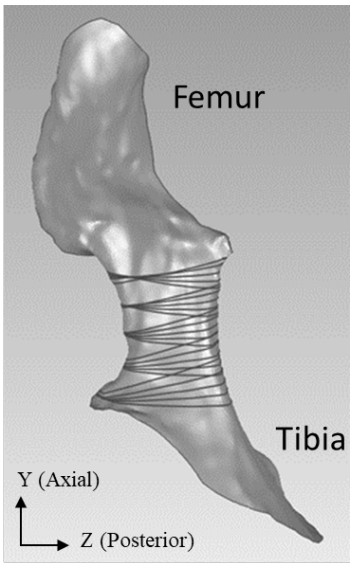

Figure 18 - Variation of 5 cross-sections with respect to the differing angles in the YZ plane.

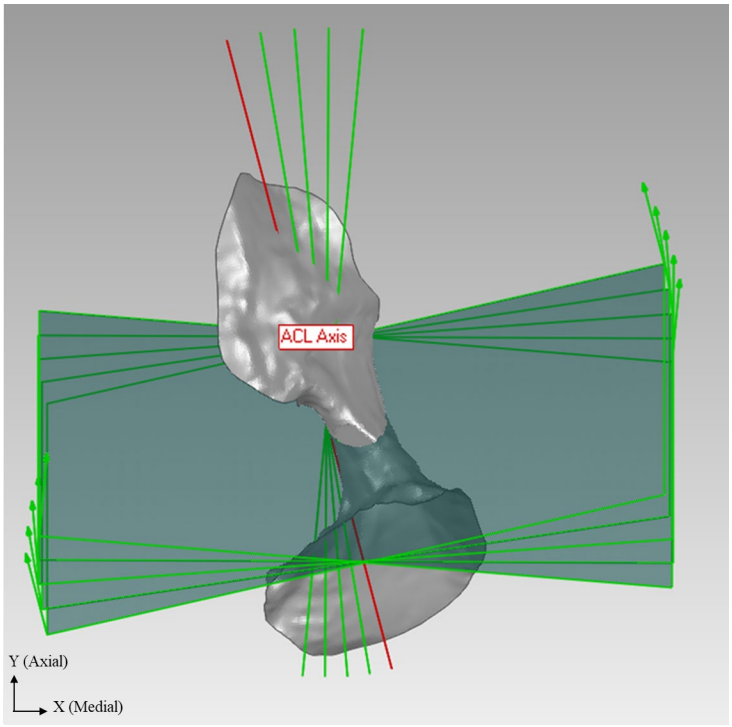

Figure 19 – Variation of planes at the middle cross-section in the XY plane.

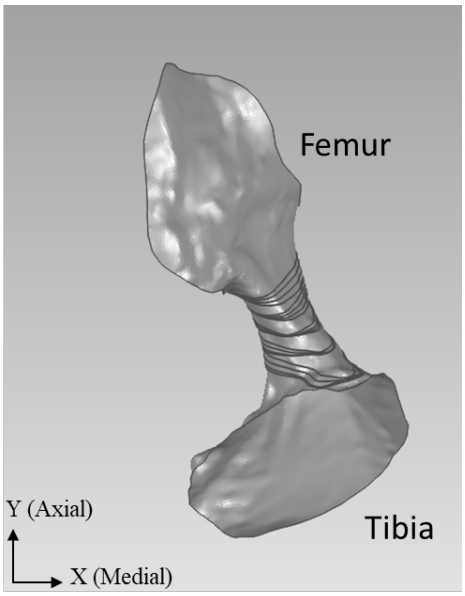

Figure 20 - Variation of 5 cross-sections with respect to the differing angles in the XY plane.

3.6 Statistical Analyses

Statistical analyses were preformed using SPSS to determine differences in cross-sectional characteristics 1) along the ACL mid-substance at each plane angle, 2) for each individual plane at each plane angle, and 3) between the major and minor axis data derived from the second moment and PCA methods. A one-way repeated measures ANOVA ($p<0.05$) was used to compare the geometric properties within the five planes determined by the original ACL Axis. ANOVA was also used to analyze the effect of adjusting the plane angles on each cross-sectional plane. The difference in each method for determining the cross-sectional axis data was compared using a t-test ($p<0.05$).

4.0 Results

Average results were obtained for each geometric category in all five planes, with Plane 1 being closest to the femur and Plane 5 being closest to the tibia, at each ACL axis angle. (Figure 21). Only 8 specimens were analyzed when varying the ACL axis in the XY direction.

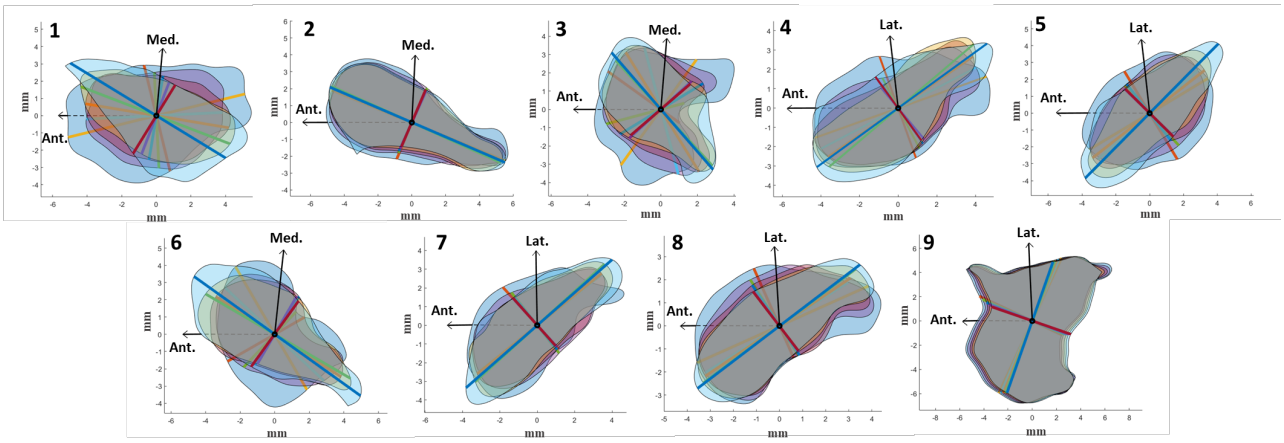

Figure 21 - Five overlaid cross-sections centered at their respective centroids based on the original ACL axis.

4.1 Cross-sections Along the Mid-substance

4.1.1 Original ACL Axis (Table 1)

For the cross-sections perpendicular to the ACL axis, the CSA of the plane closest to the tibia was significantly larger than Planes 2, 3, and 4 (Figure 22).

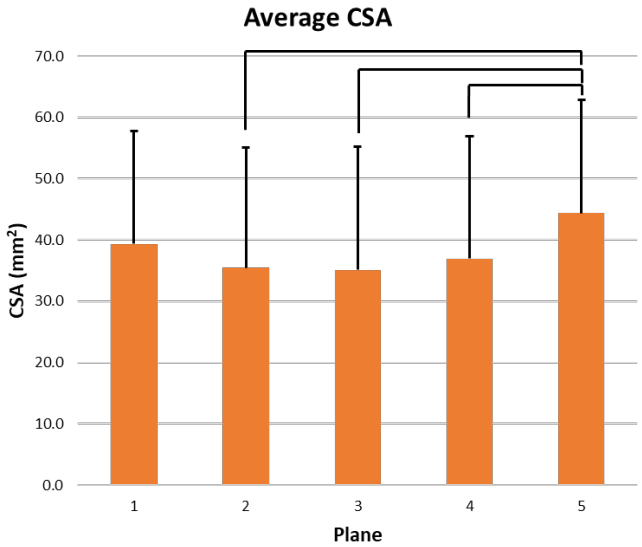

Figure 22 - Average CSA along the ACL. (-$p<0.05$)

There were no statistical differences in the values of the first principal moment, although the 2nd principal moment in Plane 5 was higher than Planes 1, 2, and 3 (Figure 23).

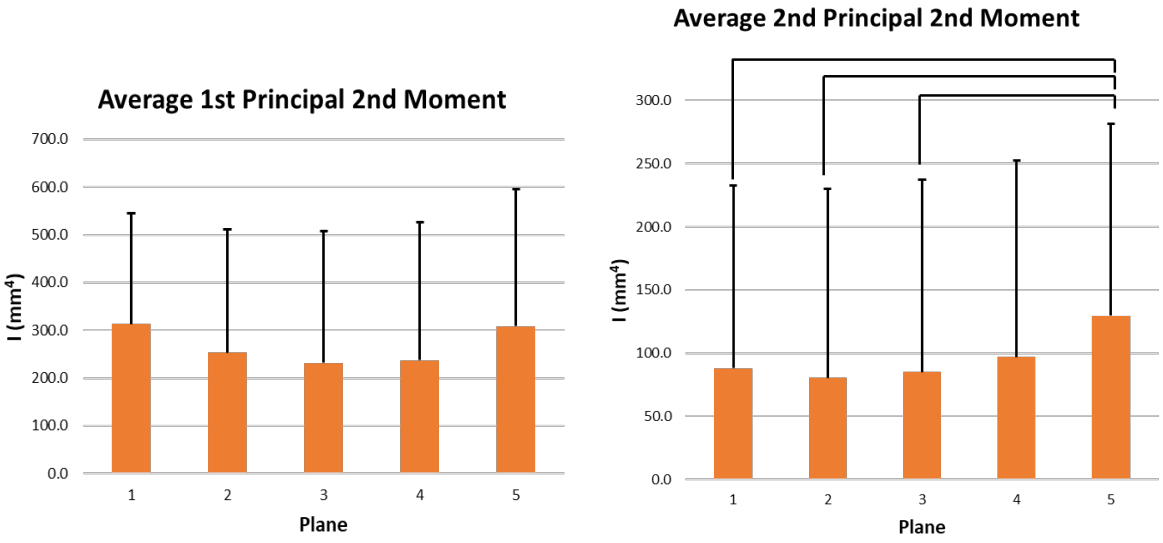

Figure 23 - Average 1st and 2nd principal moments along the ACL. (-$p<0.05$)

There was no difference observed in major axis angle between planes. Regarding major axis length, Plane 1 was longer than Planes 2-4, with Plane 2 being longer than Plane 3, and Plane 3 being longer than Plane 4. The minor axis length showed an increasing trend from Plane 1 – 5, with Plane 5 being longer than Plane 1, 2, and 4, and Plane 3 being longer than Plane 2 (Figure 24).

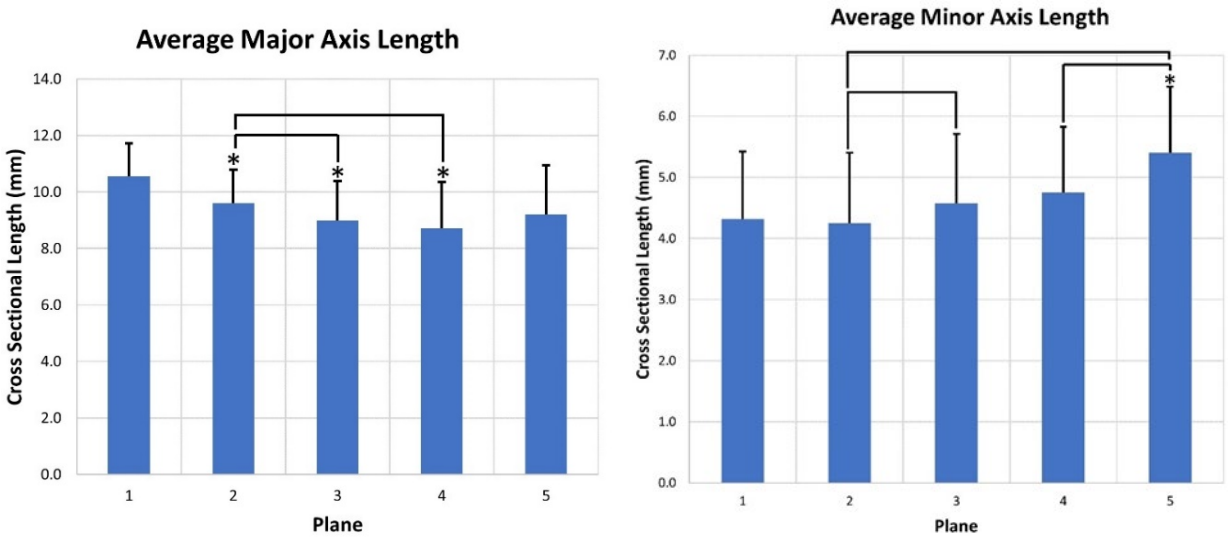

Figure 24 - Average major and minor axis lengths along the ACL. (*p<0.05 compared to Plane 1, -p<0.05 within groups)

The major-to-minor axis length ratios displayed a decreasing trend from Plane 1 – 5, with Planes 1 and 2 both being statistically different from Planes 3, 4, and 5 (Figure 25).

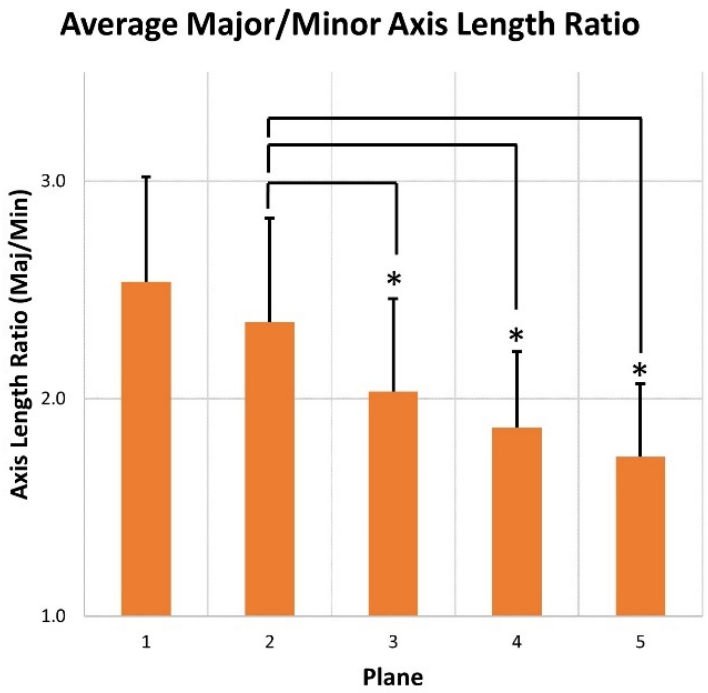

Figure 25 - Average axis length ratio along the ACL. (*p<0.05 compared to Plane 1, -p<0.05 within groups)

Table 1 - Average values for each category through all planes at 0°. (Mean ± SD)

Plane	Cross-Sectional Area (mm^2)	1st Principal 2nd Moment (mm^4)	2nd Principal 2nd Moment (mm^4)	Average Major Length (mm)	Average Minor Length (mm)	Maj/Min Axis Length Ratio	Average Major Axis Angle (deg.)
1	39.4 ± 18.4	313.2 ± 232.0	87.9 ± 144.6	10.6 ± 1.2	4.3 ± 1.1	2.5 ± 0.5	41.1 ± 13.4
2	35.4 ± 19.7	253.0 ± 258.3	80.4 ± 149.8	9.6 ± 1.2	4.3 ± 1.2	2.4 ± 0.5	39.7 ± 14.5
3	35.1 ± 20.1	231.4 ± 276.5	85.0 ± 152.2	9.0 ± 1.4	4.6 ± 1.1	2.0 ± 0.4	37.6 ± 17.3
4	36.9 ± 20.0	237.4 ± 288.1	96.8 ± 155.3	8.7 ± 1.6	4.8 ± 1.1	1.9 ± 0.3	38.5 ± 23.0
5	44.4 ± 18.5	308.3 ± 287.0	129.4 ± 152.1	9.2 ± 1.7	5.4 ± 1.1	1.7 ± 0.3	41.7 ± 39.2

4.2 Cross-sections with Respect to Variation in ACL Axes

4.2.1 Comparing the Same Plane Level between Varying Axis Angles

The effect of changing ACL axis angles from 0°-20° at each individual plane proved to be insignificant in all categories except minor axis length and major/minor axis length ratio. At Plane 4, the 20° cross-section in the YZ direction had a significantly longer minor axis length than that of the 15° cross-section. At Plane 5, the 20° minor axis length was longer than 0°, 10°, and 15°, with 15° being longer than 10° (Figure 26).

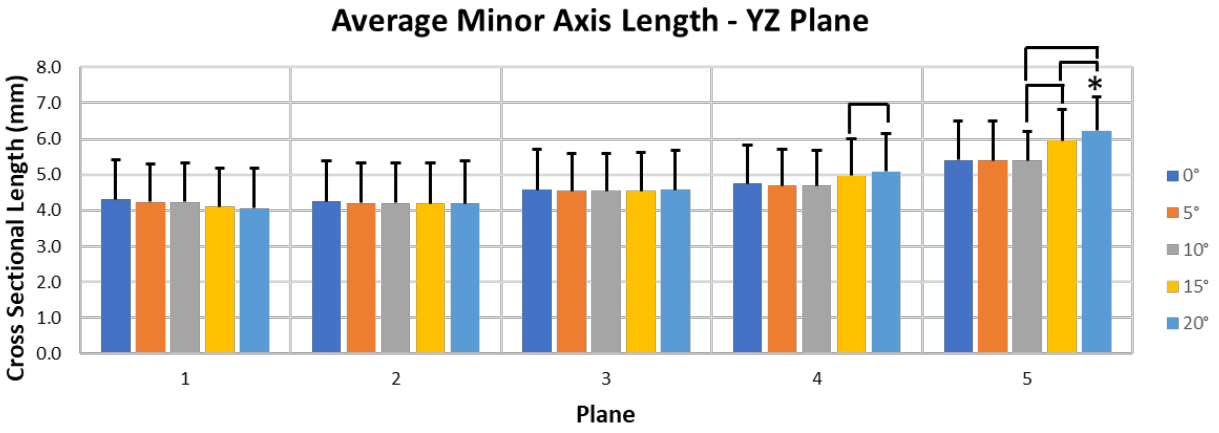

Figure 26 - Average minor axis length in the YZ plane with repect to plane angle. (*p<0.05 compared to 0°, -p<0.05 within groups)

In the XY direction, the minor length of Plane 1 was higher at 20° than 15°. At Plane 2, 15° was longer than 0° and 5°, and 20° was longer than 0°-15°. At Plane 3, 15° was longer than 0° and 5° (Figure 27).

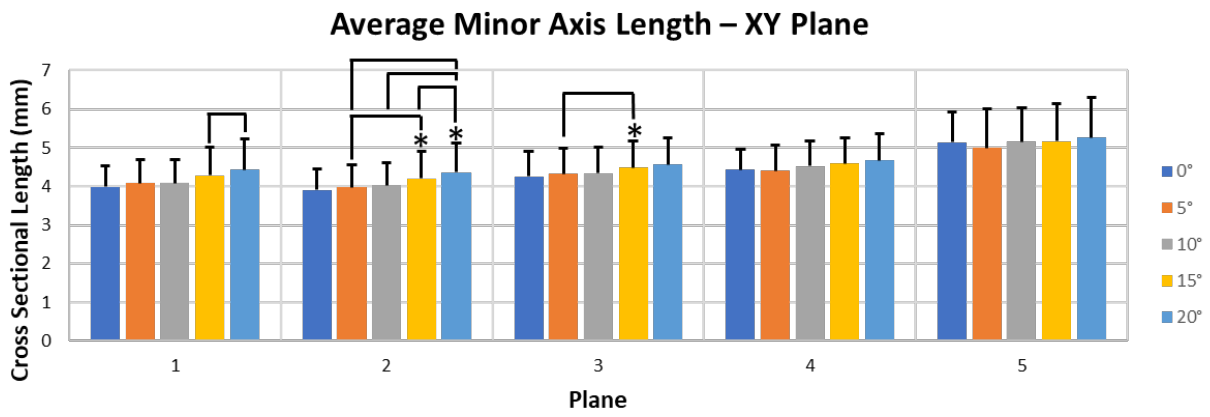

Figure 27 - Average minor axis length in the XY direction with respect to plane angle. (*p<0.05 compared to 0°, -p<0.05 within groups)

The axis length ratio was only affected by changing the plane angle in the XY direction, where the value at each plane tended to decrease as the angle increased. At Plane 1, 20° was lower than 0°, 5°, and 15°. At Plane 2, the significance pattern was identical to that of Figure 27. At Plane 3, 0° was greater than 10°-20° and 5° was greater than 15° (Figure 28).

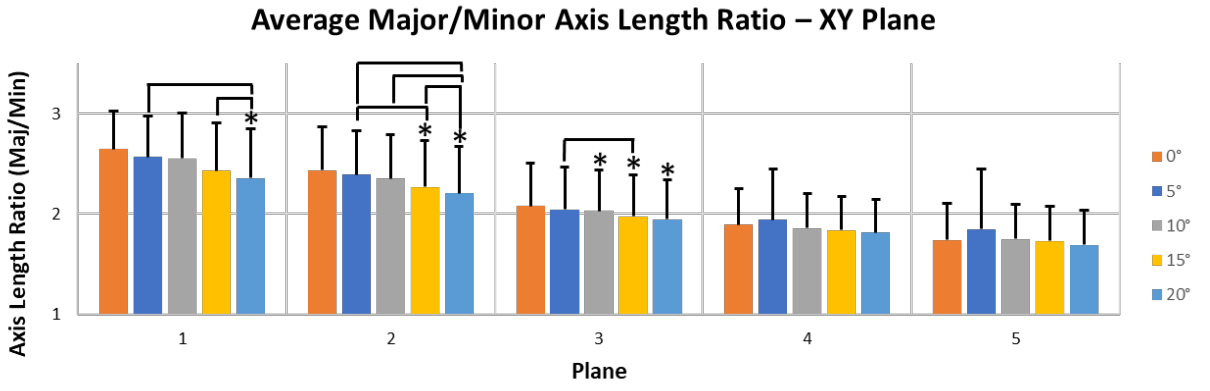

Figure 28 - Average axis length ratio in the XY direction with respect to plane angle. (*p<0.05 compared to 0°, -p<0.05 within groups)

4.2.2 Comparing Planes along the Mid-substance with Respect to One Angle (YZ Direction)

When varying the angle of the cross-sectional planes in the YZ direction, similar results were found for the CSA for each angle along the ligament. There was a slight difference at 20° with the area of Plane 5 only being larger than Planes 2 and 3 (Figure 29).

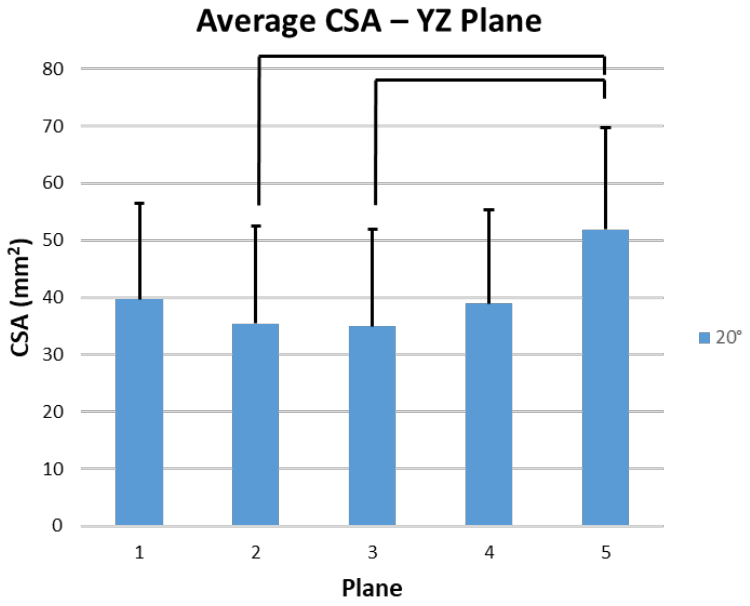

Figure 29 - Average CSA along the mid-substance in the YZ and XY planes at 20°. (*p<0.05 compared to Plane 1, -p<0.05 within groups)

For the first principal moment in the YZ direction, each angle yielded significant differences in the inner planes (2, 3 ,4) with the outer planes (1, 5), compared to no significance

at the original axis. The second principal moment trended similarly at each angle compared to the original axis, with Plane 4 being higher than 2 for 10°, 15°, 20°. Plane 4 was also higher than Plane 3 at 20° (Figure 30).

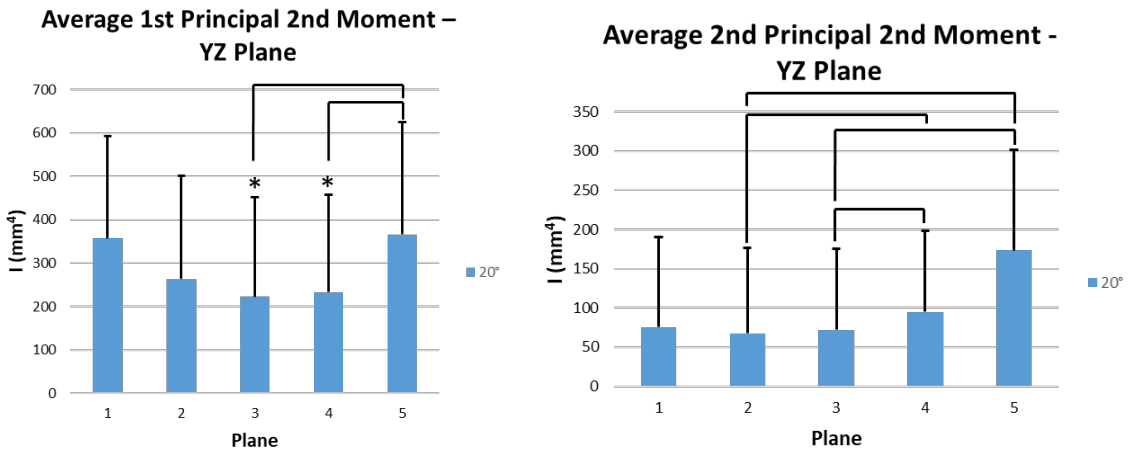

Figure 30 - Average principal moments along the mid-substance in the YZ direction at 20°.

(*$p<0.05$ compared to Plane 1, -$p<0.05$ within groups)

The major axis length data was also the same for each angle in the YZ direction compared to the original axis except at 5°, where Plane 2 and 4 were not significantly different. More differences were found in the minor axis values along the ligament at 20°, with Plane 3 being longer than Plane 2, Plane 4 being longer than Plane 1, and Plane 5 being longer than Planes 1-4 (Figure 31).

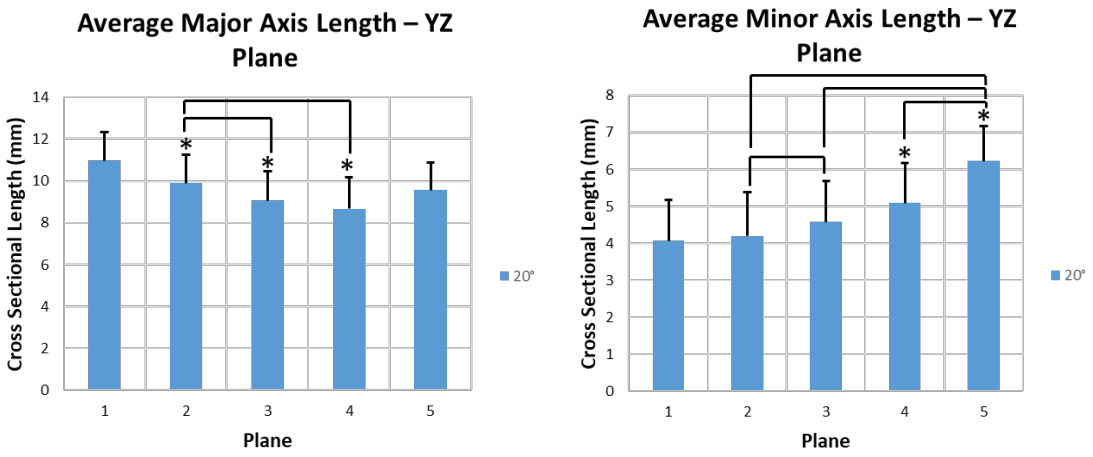

Figure 31 - Average axis lengths along the mid-substance in the YZ direction at 20°. (*p<0.05 compared to Plane 1, -p<0.05 within groups)

The major to minor axis length ratio data changed at 5° and 20° in the YZ direction. At 5°, Plane 2 is not larger than 4 and 5. At 20°, Plane 3 is also higher than Plane 5 (Figure 32).

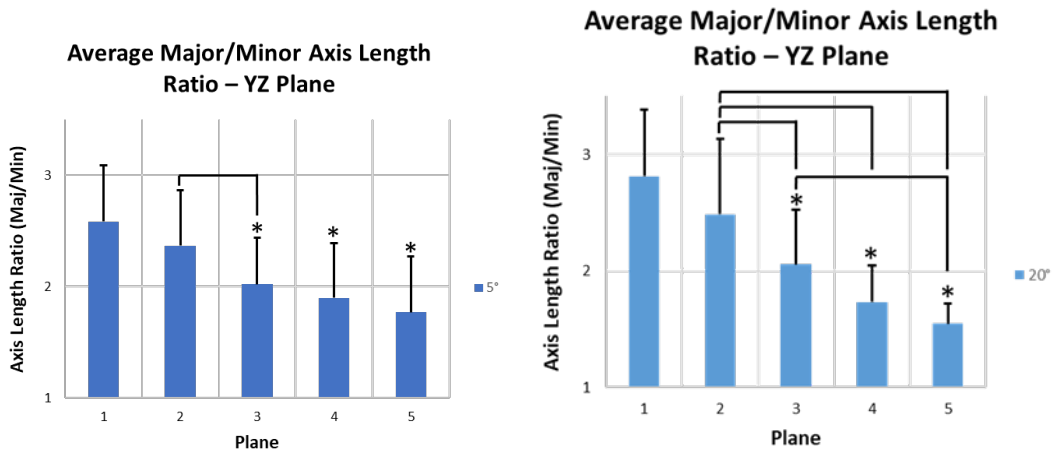

Figure 32 - Average axis length ratios along the mid-substance in the YZ direction at 5° and 20°. (*p<0.05 compared to Plane 1, -p<0.05 within groups)

The comparison of the major axis angle orientations relative to the anterior direction yielded no significant differences along the ligament regardless of plane angle. See Appendix B for more details.

4.2.3 Comparing Planes along the Mid-substance with Respect to One Angle (XY Direction)

Since the anatomy of one specimen prevented the ACL axis variation in the XY direction, the results for each angle orientation in this direction were calculated based on eight samples. The CSA at 0° and 20° yielded similar significant differences along the ligament, with Plane 1 being greater than Plane 2 at 20° (Figure 33).

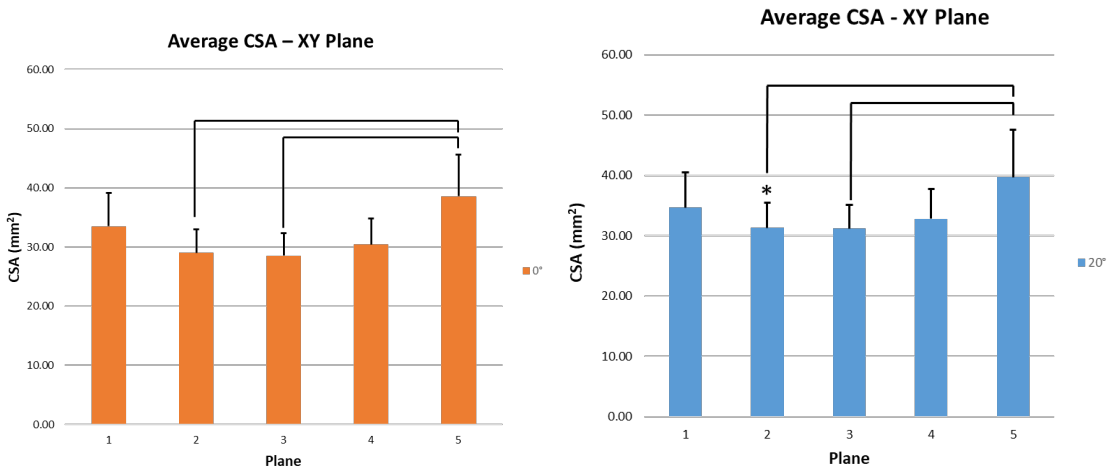

Figure 33 - Average CSA along the mid-substance in the YZ and XY directions at 20°. (*p<0.05 compared to Plane 1, -p<0.05 within groups)

The first principal moment yielded the same results at 5° and 10°, with Plane 1 being higher than Plane 3 and 4, and Plane 5 being higher than Plane 3. There were no differences along the ligament at 0°, 15°, and 20° (Figure 34).

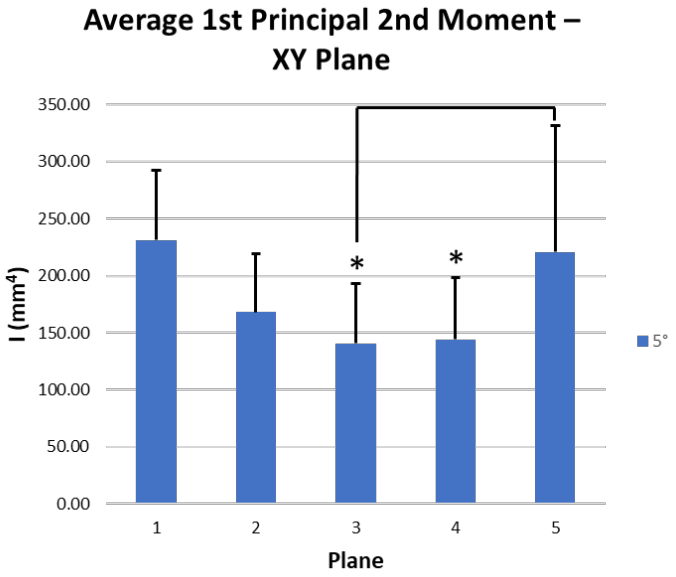

Figure 34 - Average 1st principal moment along the mid-substance in the XY direction at 5°. (*p<0.05 compared to Plane 1, -p<0.05 within groups)

Similar results were observed for the second principal moment at 5°-20°, which were slightly different than 0° (Figure 35).

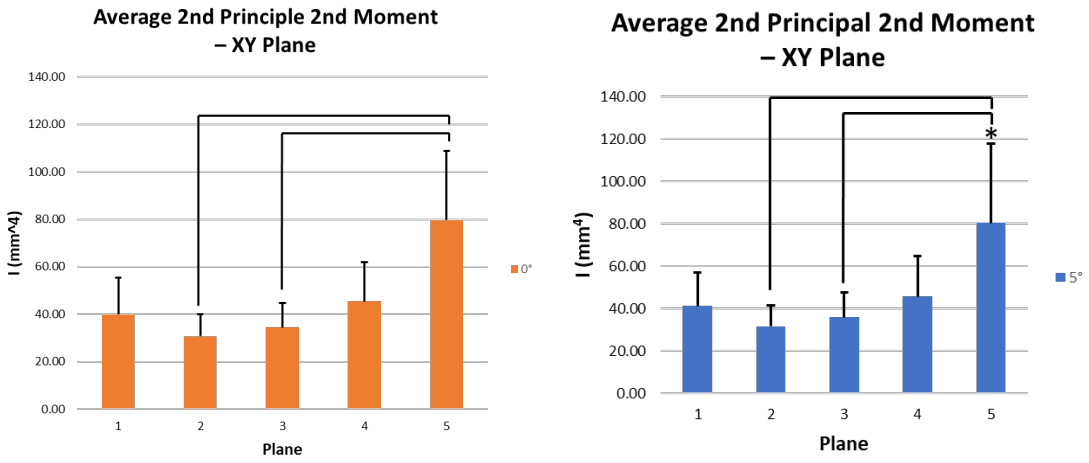

Figure 35 - Average principal moments along the mid-substance in the XY direction at 0° and 5°. (*p<0.05 compared to Plane 1, -p<0.05 within groups)

The major axis length statistical results were also identical at 5°-20°, but differed from 0° (Figure 38).

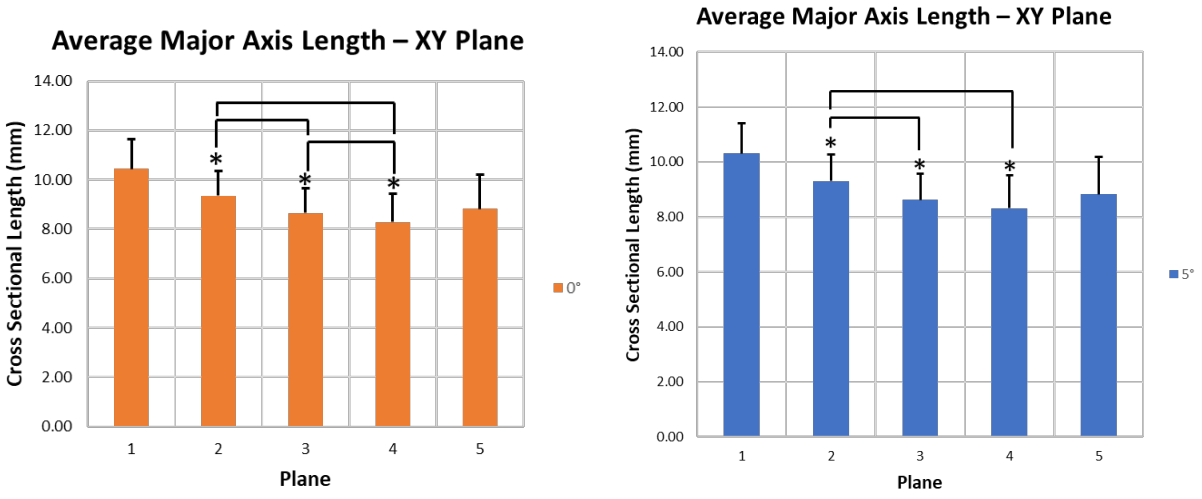

Figure 36 - Average major axis length along the mid-substance in the XY direction at 0° and 5°. (*p<0.05 compared to Plane 1, -p<0.05 within groups)

The most minor axis length differences between planes in the XY direction were found at 5°, with the only difference occurring between Planes 3 and 2 (Figure 37).

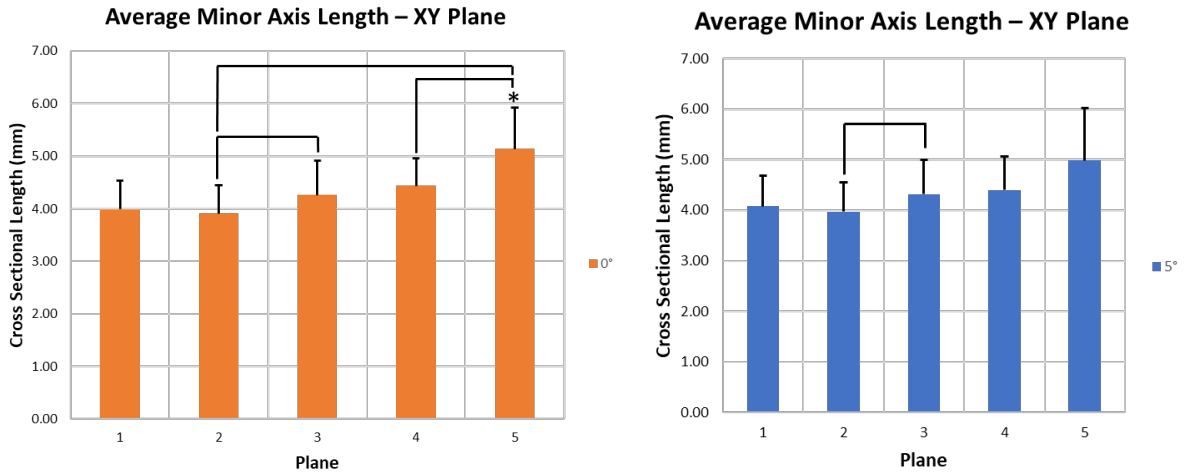

Figure 37 - Average minor axis length along the mid-substance in the XY direction at 0° and 5°. (*$p<0.05$ compared to Plane 1, -$p<0.05$ within groups)

At 20° in the XY direction, Planes 1 and 2 were no longer greater than Plane 5 (Figure 38).

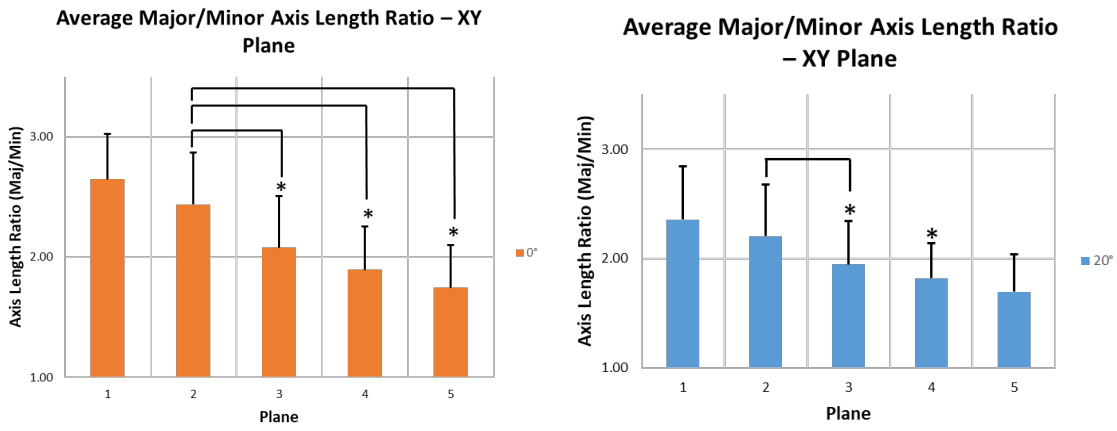

Figure 38 - Average axis length ratio along the mid-substance in the XY direction at 0° and 20°. (*p<0.05 compared to Plane 1, -p<0.05 within groups)

The major axis angle orientation relative to the anterior direction yielded no significant differences along the ligament in the XY direction.

4.3 2nd Moment vs Principal Components Analysis

Major and minor axis data was obtained using two methods: 1) finding the principal moment axes and 2) using PCA to define the principal component axes of the cross-sectional data points. There were no significant differences in major axis length, minor axis length, axis length ratios, or major axis angles between the methods (Table 2).

Table 2 – Major and minor axis data based on the 2nd moment and PCA methods of determination at 0°.

Plane	Average Major Length (mm)		Average Minor Length (mm)		Maj/Min Axis Lentgh Ratio		Average Major Axis Angle (deg.)	
	2nd Moment	PCA	2nd Moment	PCA	2nd Moment	PCA	2nd Moment	PCA
1	10.6 ± 1.2	10.6 ± 1.1	4.3 ± 1.1	4.3 ± 1.1	2.5 ± 0.5	42.0 ± 16.1	41.1 ± 13.4	42.0 ± 16.1
2	9.6 ± 1.2	9.6 ± 1.2	4.3 ± 1.2	4.2 ± 1.1	2.4 ± 0.5	40.1 ± 15.6	39.7 ± 14.5	40.1 ± 15.6
3	9.0 ± 1.4	9.0 ± 1.4	4.6 ± 1.1	4.6 ± 1.1	2.0 ± 0.4	37.4 ± 17.2	37.6 ± 17.3	37.4 ± 17.2
4	8.7 ± 1.6	8.8 ± 1.7	4.8 ± 1.1	4.8 ± 1.1	1.9 ± 0.3	37.4 ± 22.3	38.5 ± 23.0	37.4 ± 22.3
5	9.2 ± 1.7	9.3 ± 1.8	5.4 ± 1.1	5.5 ± 1.2	1.7 ± 0.3	41.1 ± 40.6	41.7 ± 39.2	41.1 ± 40.6

5.0 Conclusion

The cross-sectional properties of the ACL vary at different locations along the mid-substance. The pattern of CSA supports the "hour-glass" geometry [5] and flat mid-substance [11] described in previous studies. Fujimaki et al. and Siebold et al. reported an average CSA at the mid-substance of 39.9 ± 13.7 mm^2 and 38.7 mm^2, respectively. For the current study, the average CSA at the middle plane was 35.1 ± 20.1 mm^2.

Based on the principal moment results, the area of each cross-section is distributed farther from the major axis at planes closer to the tibia. It was also observed that the major axis does not rotate significantly along the ligament. Knowing that the AM and PL bundles twist with respect to each other, the major and minor axes do not depend on the bundle orientation.

This study yielded an average major and minor axis length of 9.0 ±1.4 mm 4.6 ± 1.1 mm, where Siebold et al. reported 9.9 mm and 3.9 mm. Closer to the center plane, the major and minor axis lengths become smaller, which would be consistent with a smaller area. The ratio of major-to-minor axis lengths tends to decrease from Plane 1 – 5, signifying a decrease in elongation, in one direction, closer to the tibial insertion. This indicates a decrease in the "ribbon"-like cross-section from the femoral to tibial insertion.

Transforming the ACL axis resulted in similar values for each quantity along the ligament, at small angles, compared to the original results. Although the average values changed depending on plane orientation, the interaction between the values at each plane did not. At 15° or 20° of variation, this conclusion is invalid seeing that the statistical differences between planes are affected.

When comparing how the ACL axis variation altered the results at each plane, changing the plane angle in the XY direction showed an effect on the minor axis length and axis length ratio at planes closest to the femur and adjusting the angle in the YZ direction effects the minor axis length at planes closest to the tibia. There were no differences in the 0° and 5° planes, so it can be concluded that cross-sectional length measurements will be impacted if the ACL axis is varied over 5°. It is safe to assume that, at larger angles, the accuracy of the major and minor axis lengths will decrease. Therefore, if the axis lengths change based on the plane angle, then the CSA and second moments would also be affected at larger angles. Although there weren't statistical differences in CSA while comparing the change in plane orientation for each individual plane, one must consider the overall structure of the ACL. If it has been shown to have an "hour-glass" structure, then oblique cross-sections may not increase area as they would for a uniform cylinder. An oblique cross-section for a cylinder would have an elliptical shape, with the minor axis length remaining constant. But for an hour-glass, an oblique cross-section would yield a Cassini oval, with a tapering of parallel surfaces to create a bicircular cross-section.

In a practical sense, when performing histological dissections or using in-vivo imaging techniques, morphometric results will be similar even if the cuts are made oblique to the anatomical axis of the ligament. It must be noted that this assumption is only valid for varying angles in two directions, and for small angle changes. If this study evaluated cross-sections at higher angular orientations, more significant differences may have surfaced.

Although the methods of principal moment and PCA for determining the major and minor axes of the cross-sections give different results, over an average of samples, the results were not statistically different. Knowing that PCA can calculate the second moment of a

boundary, the difference in axis results can be attributed to the fact that the two numerical methods are only approximations of their respective exact solutions. Nonetheless, each method is proven to be repeatable and reliable for deriving a measure of major and minor axes of the ACL mid-substance cross-section.

Appendix A Cross-Sectional Analysis MATLAB Code

```
%Written by Taylor M. Price
%Orthopaedic Engineering and Sport Medicine Laboratory
%University of Pittsburgh Swanson School of Engineering

format long

%Cooridante Change

clc;clear;
T=readtable('11_12_18_15_deg_ProbeCurves.xlsx');
[r,c]=size(T);
X=(T{1:r,{'X'1});
Y=(T{1:r,{'Y'}});
Z=(T{1:r,{'Z'}});

XD=(T{1,{'X2'}});
YD=(T{1,{'Y2'}});
ZD=(T{1,{'Z2'}});

XD2=YD;
YD2=-XD;
ZD2=0;
%New Axies
V1=[XD,YD,ZD]; %Y
V2=[XD2,YD2,ZD2];%X
V2=V2/norm(V2);
V3=cross(V2,V1);%Z
V=[V2;V1;V3]; %matrix

%Global Axies
G1=[0,1,0]; %Y
G2=[1,0,0]; %X
G3=[0,0,1]; %Z
G=[G2;G1;G3]; %matrix
```

```
for i=1:3
    for j=1:3
        Q(i,j)= dot(V(i,:),G(j,:));
    end
end

Old=[X,Y,Z];
for i=1:r
    New(i,:)=Old(i,:)*Q';
end

New_Sort=sortrows(New,2,'descend');
figure(1)
scatter3(New_Sort(:,1),New_Sort(:,2),New_Sort(:,3),'r');
hold on


xlabel('X')
ylabel('Y')
zlabel('Z')
hold off


% Extract Curves
curves=ExtractPoints(New_Sort,1000)*25.4;

%Separate Curves
curve1 =
[curves(1:length(find(curves(:,1))),1),curves(1:length(find
(curves(:,2))),2)];
curve2 =
[curves(1:length(find(curves(:,3))),3),curves(1:length(find
(curves(:,4))),4)];
curve3 =
[curves(1:length(find(curves(:,5))),5),curves(1:length(find
(curves(:,6))),6)];
curve4 =
[curves(1:length(find(curves(:,7))),7),curves(1:length(find
(curves(:,8))),8)];
curve5 =
[curves(1:length(find(curves(:,9))),9),curves(1:length(find
(curves(:,10))),10)];

%Order Points
```

```
curve1 = OrderPoints1(curve1);
curve2 = OrderPoints1(curve2);
curve3 = OrderPoints1(curve3);
curve4 = OrderPoints1(curve4);
curve5 = OrderPoints1(curve5);

%Find geometric properties of curves
[geom1,iner1,cpmo1] = polygeom( curve1(:,1),curve1(:,2) );
[geom2,iner2,cpmo2] = polygeom( curve2(:,1),curve2(:,2) );
[geom3,iner3,cpmo3] = polygeom( curve3(:,1),curve3(:,2) );
[geom4,iner4,cpmo4] = polygeom( curve4(:,1),curve4(:,2) );
[geom5,iner5,cpmo5] = polygeom( curve5(:,1),curve5(:,2) );


%Find centroids of curves
[cx1 cz1] = CentroidCalc(curve1(:,1),curve1(:,2));
[cx2 cz2] = CentroidCalc(curve2(:,1),curve2(:,2));
[cx3 cz3] = CentroidCalc(curve3(:,1),curve3(:,2));
[cx4 cz4] = CentroidCalc(curve4(:,1),curve4(:,2));
[cx5 cz5] = CentroidCalc(curve5(:,1),curve5(:,2));

%Shift Curves
curve1(:,1)= curve1(:,1)-cx1; curve1(:,2)= curve1(:,2)-cz1;
curve2(:,1)= curve2(:,1)-cx2; curve2(:,2)= curve2(:,2)-cz2;
curve3(:,1)= curve3(:,1)-cx3; curve3(:,2)= curve3(:,2)-cz3;
curve4(:,1)= curve4(:,1)-cx4; curve4(:,2)= curve4(:,2)-cz4;
curve5(:,1)= curve5(:,1)-cx5; curve5(:,2)= curve5(:,2)-cz5;

%Find length of cross section along principal axes
%Intersect = 1st pricipal moment points (distance A)
%Intersectb = 2nd principal moment points (distance B)

angle1 = atan2d(curve1(:,1),curve1(:,2));
Index1a = FindAngle(angle1,cpmo1(2)); Index1b =
FindAngle(angle1,cpmo1(2)-180);
Intersect1 = [curve1(Index1a,:);curve1(Index1b,:)];
Index1c = FindAngle(angle1,cpmo1(4)); Index1d =
FindAngle(angle1,cpmo1(4)-180);
Intersect1b = [curve1(Index1c,:);curve1(Index1d,:)];
dist1A = norm(Intersect1(1,:)-Intersect1(2,:))
dist1B = norm(Intersect1b(1,:)-Intersect1b(2,:))

angle2 = atan2d(curve2(:,1),curve2(:,2));
```

```
Index2a = FindAngle(angle2,cpmo2(2)); Index2b =
FindAngle(angle2,cpmo2(2)-180);
Intersect2 = [curve2(Index2a,:);curve2(Index2b,:)];
Index2c = FindAngle(angle2,cpmo2(4)); Index2d =
FindAngle(angle2,cpmo2(4)-180);
Intersect2b = [curve2(Index2c,:);curve2(Index2d,:)];
dist2A = norm(Intersect2(1,:)-Intersect2(2,:))
dist2B = norm(Intersect2b(1,:)-Intersect2b(2,:))

angle3 = atan2d(curve3(:,1),curve3(:,2));
Index3a = FindAngle(angle3,cpmo3(2)); Index3b =
FindAngle(angle3,cpmo3(2)-180);
Intersect3 = [curve3(Index3a,:);curve3(Index3b,:)];
Index3c = FindAngle(angle3,cpmo3(4)); Index3d =
FindAngle(angle3,cpmo3(4)-180);
Intersect3b = [curve3(Index3c,:);curve3(Index3d,:)];
dist3A = norm(Intersect3(1,:)-Intersect3(2,:))
dist3B = norm(Intersect3b(1,:)-Intersect3b(2,:))

angle4 = atan2d(curve4(:,1),curve4(:,2));
Index4a = FindAngle(angle4,cpmo4(2)); Index4b =
FindAngle(angle4,cpmo4(2)-180);
Intersect4 = [curve4(Index4a,:);curve4(Index4b,:)];
Index4c = FindAngle(angle4,cpmo4(4)); Index4d =
FindAngle(angle4,cpmo4(4)-180);
Intersect4b = [curve4(Index4c,:);curve4(Index4d,:)];
dist4A = norm(Intersect4(1,:)-Intersect4(2,:))
dist4B = norm(Intersect4b(1,:)-Intersect4b(2,:))

angle5 = atan2d(curve5(:,1),curve5(:,2));
Index5a = FindAngle(angle5,cpmo5(2)); Index5b =
FindAngle(angle5,cpmo5(2)-180);
Intersect5 = [curve5(Index5a,:);curve5(Index5b,:)];
Index5c = FindAngle(angle5,cpmo5(4)); Index5d =
FindAngle(angle5,cpmo5(4)-180);
Intersect5b = [curve5(Index5c,:);curve5(Index5d,:)];
dist5A = norm(Intersect5(1,:)-Intersect5(2,:))
dist5B = norm(Intersect5b(1,:)-Intersect5b(2,:))

%Find length of cross section using PCA
%Intersect = 1st priciple moment points (distance A)
%Intersectb = 2nd principal moment points (distance B)

X = {curve1,curve2,curve3,curve4,curve5};
```

```
sizecurves = size(curve1);
h = ones(sizecurves(1),1);

%Normalize
for i = 1:5
    for j = 1:sizecurves(2)
    u(i,j) = sum(X{i}(:,j))/sizecurves(1);
    end
end

for i = 1:5
Xnormal{i} = X{i}-h*u(i,:);
end

%Covariance Matrix
%CoVar = (1/(sizeX(1)-1))*Xnormal'*Xnormal
for i = 1:5
CoVar{i} = cov(Xnormal{i});
end

% Singular Value Decomposition
[vec1 val1] = eig(CoVar{1});
[vec2 val2] = eig(CoVar{2});
[vec3, val3] = eig(CoVar{3});
[vec4 val4] = eig(CoVar{4});
[vec5 val5] = eig(CoVar{5});

PCA_Axis11 = vec1(:,1);PCA_Axis12 = vec1(:,2);
PCA_Axis21 = vec2(:,1);PCA_Axis22 = vec2(:,2);
PCA_Axis31 = vec3(:,1);PCA_Axis32 = vec3(:,2);
PCA_Axis41 = vec4(:,1);PCA_Axis42 = vec4(:,2);
PCA_Axis51 = vec5(:,1);PCA_Axis52 = vec5(:,2);

ang11a = atan2( vec1(1,2), vec1(2,2) ); ang12a = atan2(
vec1(1,1), vec1(2,1) );
ang12 = rad2deg(ang11a+(ang11a < 0)*pi); ang11 =
rad2deg(ang12a+(ang12a < 0)*pi);
[ang11 ang12]

ang21a = atan2( vec2(1,2), vec2(2,2) ); ang22a = atan2(
vec2(1,1), vec2(2,1) );
ang22 = rad2deg(ang21a+(ang21a < 0)*pi); ang21 =
rad2deg(ang22a+(ang22a < 0)*pi);
[ang21 ang22]
```

```
ang31a = atan2( vec3(1,2), vec3(2,2) ); ang32a = atan2(
vec3(1,1), vec3(2,1) );
ang32 = rad2deg(ang31a+(ang31a < 0)*pi); ang31 =
rad2deg(ang32a+(ang32a < 0)*pi);
[ang31 ang32]

ang41a = atan2( vec4(1,2), vec4(2,2) ); ang42a = atan2(
vec4(1,1), vec4(2,1) );
ang42 = rad2deg(ang41a+(ang41a < 0)*pi); ang41 =
rad2deg(ang42a+(ang42a < 0)*pi);
[ang41 ang42]

ang51a = atan2( vec5(1,2), vec5(2,2) ); ang52a = atan2(
vec5(1,1), vec5(2,1) );
ang52 = rad2deg(ang51a+(ang51a < 0)*pi); ang51 =
rad2deg(ang52a+(ang52a < 0)*pi);
[ang51 ang52]

%Plot PCA Axes
x11 = [-PCA_Axis11(1) 0 PCA_Axis11(1)]; z11 = [-
PCA_Axis11(2) 0 PCA_Axis11(2)];
x12 = [-PCA_Axis12(1) 0 PCA_Axis12(1)]; z12 = [-
PCA_Axis12(2) 0 PCA_Axis12(2)];

x21 = [-PCA_Axis21(1) 0 PCA_Axis21(1)]; z21 = [-
PCA_Axis21(2) 0 PCA_Axis21(2)];
x22 = [-PCA_Axis22(1) 0 PCA_Axis22(1)]; z22 = [-
PCA_Axis22(2) 0 PCA_Axis22(2)];

x31 = [-PCA_Axis31(1) 0 PCA_Axis31(1)]; z31 = [-
PCA_Axis31(2) 0 PCA_Axis31(2)];
x32 = [-PCA_Axis32(1) 0 PCA_Axis32(1)]; z32 = [-
PCA_Axis32(2) 0 PCA_Axis32(2)];

x41 = [-PCA_Axis41(1) 0 PCA_Axis41(1)]; z41 = [-
PCA_Axis41(2) 0 PCA_Axis41(2)];
x42 = [-PCA_Axis42(1) 0 PCA_Axis42(1)]; z42 = [-
PCA_Axis42(2) 0 PCA_Axis42(2)];

x51 = [-PCA_Axis51(1) 0 PCA_Axis51(1)]; z51 = [-
PCA_Axis51(2) 0 PCA_Axis51(2)];
x52 = [-PCA_Axis52(1) 0 PCA_Axis52(1)]; z52 = [-
PCA_Axis52(2) 0 PCA_Axis52(2)];
```

```
%Find PCA distances
Index1a = FindAngle(angle1,ang11); Index1b =
FindAngle(angle1,ang11-180);
PCAIntersect1 = [curve1(Index1a,:);curve1(Index1b,:)];
Index1c = FindAngle(angle1,ang12); Index1d =
FindAngle(angle1,ang12-180);
PCAIntersect1b = [curve1(Index1c,:);curve1(Index1d,:)];
PCAdist1A = norm(PCAIntersect1(1,:)-PCAIntersect1(2,:));
PCAdist1B = norm(PCAIntersect1b(1,:)-PCAIntersect1b(2,:));

Index2a = FindAngle(angle2,ang21); Index2b =
FindAngle(angle2,ang21-180);
PCAIntersect2 = [curve2(Index2a,:);curve2(Index2b,:)];
Index2c = FindAngle(angle2,ang22); Index2d =
FindAngle(angle2,ang22-180);
PCAIntersect2b = [curve2(Index2c,:);curve2(Index2d,:)];
PCAdist2A = norm(PCAIntersect2(1,:)-PCAIntersect2(2,:));
PCAdist2B = norm(PCAIntersect2b(1,:)-PCAIntersect2b(2,:));

Index3a = FindAngle(angle3,ang31); Index3b =
FindAngle(angle3,ang31-180);
PCAIntersect3 = [curve3(Index3a,:);curve3(Index3b,:)];
Index3c = FindAngle(angle3,ang32); Index3d =
FindAngle(angle3,ang32-180);
PCAIntersect3b = [curve3(Index3c,:);curve3(Index3d,:)];
PCAdist3A = norm(PCAIntersect3(1,:)-PCAIntersect3(2,:));
PCAdist3B = norm(PCAIntersect3b(1,:)-PCAIntersect3b(2,:));

Index4a = FindAngle(angle4,ang41); Index4b =
FindAngle(angle4,ang41-180);
PCAIntersect4 = [curve4(Index4a,:);curve4(Index4b,:)];
Index4c = FindAngle(angle4,ang42); Index4d =
FindAngle(angle4,ang42-180);
PCAIntersect4b = [curve4(Index4c,:);curve4(Index4d,:)];
PCAdist4A = norm(PCAIntersect4(1,:)-PCAIntersect4(2,:));
PCAdist4B = norm(PCAIntersect4b(1,:)-PCAIntersect4b(2,:));

Index5a = FindAngle(angle5,ang51); Index5b =
FindAngle(angle5,ang51-180);
PCAIntersect5 = [curve5(Index5a,:);curve5(Index5b,:)];
Index5c = FindAngle(angle5,ang52); Index5d =
FindAngle(angle5,ang52-180);
```

```
PCAIntersect5b = [curve5(Index5c,:);curve5(Index5d,:)];
PCAdist5A = norm(PCAIntersect5(1,:)-PCAIntersect5(2,:));
PCAdist5B = norm(PCAIntersect5b(1,:)-PCAIntersect5b(2,:));

%transform global AP and ML axes (Z and X) onto local axis
ptsAP = [0 0 0; 0 0 -6];
ptsML = [0 0 0; -4 0 0];

for i=1:2
    NewptsAP(i,:)=ptsAP(i,:)*Q';
    NewptsML(i,:)=ptsML(i,:)*Q';
end
NewptsAP;
NewptsML;

%Define AP and ML axes on plots
angleAP = atan2d(NewptsAP(2,1), NewptsAP(2,3)); angleML =
atan2d(NewptsML(2,1), NewptsML(2,3));
IndexAP1 = FindAngle(angle1,angleAP); IndexML1 =
FindAngle(angle1,angleML);
IntersectAP1 = curve1(IndexAP1,:); IntersectML1 =
curve1(IndexML1,:);

IndexAP2 = FindAngle(angle2,angleAP); IndexML2 =
FindAngle(angle2,angleML);
IntersectAP2 = curve2(IndexAP2,:); IntersectML2 =
curve2(IndexML2,:);

IndexAP3 = FindAngle(angle3,angleAP); IndexML3 =
FindAngle(angle3,angleML);
IntersectAP3 = curve3(IndexAP3,:); IntersectML3 =
curve3(IndexML3,:);

IndexAP4 = FindAngle(angle4,angleAP); IndexML4 =
FindAngle(angle4,angleML);
IntersectAP4 = curve4(IndexAP4,:); IntersectML4 =
curve4(IndexML4,:);

IndexAP5 = FindAngle(angle5,angleAP); IndexML5 =
FindAngle(angle5,angleML);
IntersectAP5 = curve5(IndexAP5,:); IntersectML5 =
curve5(IndexML5,:);
```

```
%Display 1st Principal 2nd Moment Axes
P1z1 = [Intersect1(1,2) Intersect1(2,2)];P1x1 =
[Intersect1(1,1) Intersect1(2,1)];
P1z2 = [Intersect2(1,2) Intersect2(2,2)];P1x2 =
[Intersect2(1,1) Intersect2(2,1)];
P1z3 = [Intersect3(1,2) Intersect3(2,2)];P1x3 =
[Intersect3(1,1) Intersect3(2,1)];
P1z4 = [Intersect4(1,2) Intersect4(2,2)];P1x4 =
[Intersect4(1,1) Intersect4(2,1)];
P1z5 = [Intersect5(1,2) Intersect5(2,2)];P1x5 =
[Intersect5(1,1) Intersect5(2,1)];

%Display 2nd Principal 2nd Moment Axes

P2z1 = [Intersect1b(1,2) Intersect1b(2,2)];P2x1 =
[Intersect1b(1,1) Intersect1b(2,1)];
P2z2 = [Intersect2b(1,2) Intersect2b(2,2)];P2x2 =
[Intersect2b(1,1) Intersect2b(2,1)];
P2z3 = [Intersect3b(1,2) Intersect3b(2,2)];P2x3 =
[Intersect3b(1,1) Intersect3b(2,1)];
P2z4 = [Intersect4b(1,2) Intersect4b(2,2)];P2x4 =
[Intersect4b(1,1) Intersect4b(2,1)];
P2z5 = [Intersect5b(1,2) Intersect5b(2,2)];P2x5 =
[Intersect5b(1,1) Intersect5b(2,1)];

%Display PCA Minor Axis
PCA1z1 = [PCAIntersect1(1,2) PCAIntersect1(2,2)];PCA1x1 =
[PCAIntersect1(1,1) PCAIntersect1(2,1)];
PCA1z2 = [PCAIntersect2(1,2) PCAIntersect2(2,2)];PCA1x2 =
[PCAIntersect2(1,1) PCAIntersect2(2,1)];
PCA1z3 = [PCAIntersect3(1,2) PCAIntersect3(2,2)];PCA1x3 =
[PCAIntersect3(1,1) PCAIntersect3(2,1)];
PCA1z4 = [PCAIntersect4(1,2) PCAIntersect4(2,2)];PCA1x4 =
[PCAIntersect4(1,1) PCAIntersect4(2,1)];
PCA1z5 = [PCAIntersect5(1,2) PCAIntersect5(2,2)];PCA1x5 =
[PCAIntersect5(1,1) PCAIntersect5(2,1)];

%Display PCA Major Axis
PCA2z1 = [PCAIntersect1b(1,2) PCAIntersect1b(2,2)];PCA2x1 =
[PCAIntersect1b(1,1) PCAIntersect1b(2,1)];
PCA2z2 = [PCAIntersect2b(1,2) PCAIntersect2b(2,2)];PCA2x2 =
[PCAIntersect2b(1,1) PCAIntersect2b(2,1)];
PCA2z3 = [PCAIntersect3b(1,2) PCAIntersect3b(2,2)];PCA2x3 =
[PCAIntersect3b(1,1) PCAIntersect3b(2,1)];
```

```
PCA2z4 = [PCAIntersect4b(1,2) PCAIntersect4b(2,2)];PCA2x4 =
[PCAIntersect4b(1,1) PCAIntersect4b(2,1)];
PCA2z5 = [PCAIntersect5b(1,2) PCAIntersect5b(2,2)];PCA2x5 =
[PCAIntersect5b(1,1) PCAIntersect5b(2,1)];

%Plot results

figure(2)

plot(polyshape(curve1(:,2),curve1(:,1)))
hold on
plot([0 IntersectAP1(2)],[0 IntersectAP1(1)],'k--
','LineWidth',1); plot([IntersectAP1(2)
NewptsAP(2,3)],[IntersectAP1(1)
NewptsAP(2,1)],'k','LineWidth',2)
plot([0 IntersectML1(2)],[0 IntersectML1(1)],'k--
','LineWidth',1); plot([IntersectML1(2)
NewptsML(2,3)],[IntersectML1(1)
NewptsML(2,1)],'k','LineWidth',2)
hold on;p1 = plot(P1z1,P1x1,'LineWidth',4);
hold on;p2 = plot(P2z1,P2x1,'LineWidth',4);
hold on;pca1 = plot(PCA1z1,PCA1x1,'LineWidth',3);
hold on;pca2 = plot(PCA2z1,PCA2x1,'LineWidth',3);
hold on;p3 = scatter(0,0,'LineWidth',3);
legend([p3,p1,p2,pca1,pca2],{'Centroid','1st Principal
Moment Axis','2nd Principal Moment Axis','PCA Minor
Axis','PCA Major Axis'})
title('Curve 1')
axis equal

figure(3)

plot(polyshape(curve2(:,2),curve2(:,1)))
hold on
plot([0 IntersectAP2(2)],[0 IntersectAP2(1)],'k--
','LineWidth',1); plot([IntersectAP2(2)
NewptsAP(2,3)],[IntersectAP2(1)
NewptsAP(2,1)],'k','LineWidth',2)
plot([0 IntersectML2(2)],[0 IntersectML2(1)],'k--
','LineWidth',1); plot([IntersectML2(2)
NewptsML(2,3)],[IntersectML2(1)
NewptsML(2,1)],'k','LineWidth',2)
hold on;p1 = plot(P1z2,P1x2,'LineWidth',4);
hold on;p2 = plot(P2z2,P2x2,'LineWidth',4);
```

```
hold on;pca1 = plot(PCA1z2,PCA1x2,'LineWidth',3);
hold on;pca2 = plot(PCA2z2,PCA2x2,'LineWidth',3);
hold on;p3 = scatter(0,0,'LineWidth',3);
legend([p3,p1,p2,pca1,pca2],{'Centroid','1st Principal
Moment Axis','2nd Principal Moment Axis','PCA Minor
Axis','PCA Major Axis'})
title('Curve 2')
axis equal

figure(4)

plot(polyshape(curve3(:,2),curve3(:,1)))
hold on
plot([0 IntersectAP3(2)],[0 IntersectAP3(1)],'k--
','LineWidth',1); plot([IntersectAP3(2)
NewptsAP(2,3)],[IntersectAP3(1)
NewptsAP(2,1)],'k','LineWidth',2
plot([0 IntersectML3(2)],[0 IntersectML3(1)],'k--
','LineWidth',1); plot([IntersectML3(2)
NewptsML(2,3)],[IntersectML3(1)
NewptsML(2,1)],'k','LineWidth',2
hold on;p1 = plot(P1z3,P1x3,'LineWidth',4);
hold on;p2 = plot(P2z3,P2x3,'LineWidth',4);
hold on;pca1 = plot(PCA1z3,PCA1x3,'LineWidth',3);
hold on;pca2 = plot(PCA2z3,PCA2x3,'LineWidth',3);
hold on;p3 = scatter(0,0,'LineWidth',3);
legend([p3,p1,p2,pca1,pca2],{'Centroid','1st Principal
Moment Axis','2nd Principa Moment Axis','PCA Minor
Axis','PCA Major Axis'})
title('Curve 3')
axis equal

figure(5)

plot(polyshape(curve4(:,2),curve4(:,1)))
hold on
plot([0 IntersectAP4(2)],[0 IntersectAP4(1)],'k--
','LineWidth',1); plot([IntersectAP4(2)
NewptsAP(2,3)],[IntersectAP4(1)
NewptsAP(2,1)],'k','LineWidth',2
plot([0 IntersectML4(2)],[0 IntersectML4(1)],'k--
','LineWidth',1); plot([IntersectML4(2)
NewptsML(2,3)],[IntersectML4(1)
NewptsML(2,1)],'k','LineWidth',2)
```

```
hold on;p1 = plot(P1z4,P1x4,'LineWidth',4);
hold on;p2 = plot(P2z4,P2x4,'LineWidth',4);
hold on;pca1 = plot(PCA1z4,PCA1x4,'LineWidth',3);
hold on;pca2 = plot(PCA2z4,PCA2x4,'LineWidth',3);
hold on;p3 = scatter(0,0,'LineWidth',3);
legend([p3,p1,p2,pca1,pca2],{'Centroid','1st Principal
Moment Axis','2nd Principal Moment Axis','PCA Minor
Axis','PCA Major Axis'})
title('Curve 4')
axis equal

figure(6)

plot(polyshape(curve5(:,2),curve5(:,1)))
hold on
plot([0 IntersectAP5(2)],[0 IntersectAP5(1)],'k--
','LineWidth',1); plot([IntersectAP5(2)
NewptsAP(2,3)],[IntersectAP5(1)
NewptsAP(2,1)],'k','LineWidth',2
plot([0 IntersectML5(2)],[0 IntersectML5(1)],'k--
','LineWidth',1); plot([IntersectML5(2)
NewptsML(2,3)],[IntersectML5(1)
NewptsML(2,1)],'k','LineWidth',2
hold on;p1 = plot(P1z5,P1x5,'LineWidth',4);
hold on;p2 = plot(P2z5,P2x5,'LineWidth',4);
hold on;pca1 = plot(PCA1z5,PCA1x5,'LineWidth',3);
hold on;pca2 = plot(PCA2z5,PCA2x5,'LineWidth',3);
hold on;p3 = scatter(0,0,'LineWidth',3);
legend([p3,p1,p2,pca1,pca2],{'Centroid','1st Principal
Moment Axis','2nd Principal Moment Axis','PCA Minor
Axis','PCA Major Axis'})
title('Curve 5')
axis equal

figure(7)
plot(polyshape(curve5(:,2),curve5(:,1))); hold on
plot([0 IntersectAP5(2)],[0 IntersectAP5(1)],'k--
','LineWidth',1); plot([IntersectAP5(2)
NewptsAP(2,3)],[IntersectAP5(1)
NewptsAP(2,1)],'k','LineWidth',2
p51 = plot(P1z5,P1x5,'LineWidth',4); hold on
p52 = plot(P2z5,P2x5,'LineWidth',4); hold on
plot(polyshape(curve4(:,2),curve4(:,1))); hold on
p41 = plot(P1z4,P1x4,'LineWidth',4); hold on
```

```
p42 = plot(P2z4,P2x4,'LineWidth',4); hold on
plot(polyshape(curve3(:,2),curve3(:,1))); hold on
p31 = plot(P1z3,P1x3,'LineWidth',4); hold on
p32 = plot(P2z3,P2x3,'LineWidth',4); hold on
plot(polyshape(curve2(:,2),curve2(:,1))); hold on
p21 = plot(P1z2,P1x2,'LineWidth',4); hold on
p22 = plot(P2z2,P2x2,'LineWidth',4); hold on
plot(polyshape(curve1(:,2),curve1(:,1))); hold on
p11 = plot(P1z1,P1x1,'LineWidth',4); hold on
p12 = plot(P2z1,P2x1,'LineWidth',4); hold on
plot([0 IntersectML5(2)],[0
IntersectML5(1)],'k','LineWidth',2); plot([IntersectML5(2)
NewptsML(2,3)],[IntersectML5(1)
NewptsML(2,1)],'k','LineWidth',2)
hold on
p3 = scatter(0,0,'k','LineWidth',3);
legend([p3,p11,p21,p31,p41,p51],{'Centroid','1st Principal
Axis - Plane 1','1st Principal Axis - Plane 2','1st
Principal Axis - Plane 3','1st Principal Axis - Plane
4','1st Principal Axis - Plane 5'})
axis equal


format short
MomentAngles2 = [cpmo1(2) cpmo1(4)
                 cpmo2(2) cpmo2(4)
                 cpmo3(2) cpmo3(4)
                 cpmo4(2) cpmo4(4)
                 cpmo5(2) cpmo5(4)]

PCAAngles = [ang11 ang12
             ang21 ang22
             ang31 ang32
             ang41 ang42
             ang51 ang52]

Areas2 = [geom1(1);geom2(1);geom3(1);geom4(1);geom5(1)]
%mm^2
format long
SecondMoments2 = [cpmo1(1) cpmo1(3)
                  cpmo2(1) cpmo2(3)
                  cpmo3(1) cpmo3(3)
                  cpmo4(1) cpmo4(3)
                  cpmo5(1) cpmo5(3)] %mm^4
```

```
MajMinAxes_2ndMoment = [dist1A dist1B
                        dist2A dist2B
                        dist3A dist3B
                        dist4A dist4B
                        dist5A dist5B]

MajMinAxes_PCA = [PCAdist1A PCAdist1B
                  PCAdist2A PCAdist2B
                  PCAdist3A PCAdist3B
                  PCAdist4A PCAdist4B
                  PCAdist5A PCAdist5B]
```

Appendix A.1 MATLAB Function "ExtractPoints"

```
function Curves = ExtractPoints(Array,NumPoints)

pts = NumPoints;
New_Sort = Array;
CurveChange = find(ischange(New_Sort(:,2)));
j = 1;
i = 1;
k = 0;
for j = 1:length(CurveChange)+1
    %Every Curve Except Last Curve
    if j <= length(CurveChange)
        while i<CurveChange(j)
           curves(k+1,(j*2)-1)=New_Sort(i,1);
           curves(k+1,(j*2))=New_Sort(i,3);
           curves(pts,:)=0;
           i = i+1;
           k = k+1;
        end
            k = 0;

    else
        %Last Curve
        while i <= length(New_Sort)
```

```
            curves(k+1,(j*2)-1)=New_Sort(i,1);
            curves(k+1,(j*2))=New_Sort(i,3);
            curves(pts,:)=0;
            i = i+1;
            k = k+1;
        end

    end


end
Curves = curves;
```

Appendix A.2 MATLAB Function "OrderPoints1"

```
function OrderedCurve = OrderPoints1(x)

% dist = [x(1,1)-x(2,1),x(1,2)-x(2,2)]; %Distance Between
First Coordinates
% pointdistance(1,:) = sqrt(dist(1)^2 + dist(2)^2);
%Distance Between first points
OrderedCurve(1,:) = x(1,:); %Starting point
for i = 1:length(x)-1

   for j = i+1:length(x)

dist = [x(i,1)-x(j,1),x(i,2)-x(j,2)];
pointdistance(i,j-1) = sqrt(dist(1)^2 + dist(2)^2);
   end
 [M I] = min(pointdistance(i,i:end));

 element = x(i+1,:);
 OrderedCurve(i+1,:) = x(i+I,:);
 x(i+1,:) = x(i+I,:);
 x(i+I,:) = element;


end
```

Appendix A.3 MATLAB Function "polygeom" [13]

```
function [ geom, iner, cpmo ] = polygeom( x, y )
%POLYGEOM Geometry of a planar polygon
%
%   POLYGEOM( X, Y ) returns area, X centroid,
%   Y centroid and perimeter for the planar polygon
%   specified by vertices in vectors X and Y.
%
%   [ GEOM, INER, CPMO ] = POLYGEOM( X, Y ) returns
%   area, centroid, perimeter and area moments of
%   inertia for the polygon.
%   GEOM = [ area   X_cen  Y_cen  perimeter ]
%   INER = [ Ixx    Iyy    Ixy    Iuu    Ivv    Iuv ]
%     u,v are centroidal axes parallel to x,y axes.
%   CPMO = [ I1     ang1   I2     ang2   J ]
%     I1,I2 are centroidal principal moments about axes
%         at angles ang1,ang2.
%     ang1 and ang2 are in radians.
%     J is centroidal polar moment.  J = I1 + I2 = Iuu +
Ivv

% H.J. Sommer III - 16.12.09 - tested under MATLAB v9.0
%
% sample data
% x = [ 2.000  0.500  4.830  6.330 ]';
% y = [ 4.000  6.598  9.098  6.500 ]';
% 3x5 test rectangle with long axis at 30 degrees
% area=15, x_cen=3.415, y_cen=6.549, perimeter=16
% Ixx=659.561, Iyy=201.173, Ixy=344.117
% Iuu=16.249, Ivv=26.247, Iuv=8.660
% I1=11.249, ang1=30deg, I2=31.247, ang2=120deg, J=42.496
%
% H.J. Sommer III, Ph.D., Professor of Mechanical
Engineering, 337 Leonhard Bldg
% The Pennsylvania State University, University Park, PA
16802
% (814)863-8997  FAX (814)865-9693  hjs1-at-psu.edu
www.mne.psu.edu/sommer/

% begin function POLYGEOM
```

```
% check if inputs are same size
if ~isequal( size(x), size(y) ),
  error( 'X and Y must be the same size');
end

% temporarily shift data to mean of vertices for improved
accuracy
xm = mean(x);
ym = mean(y);
x = x - xm;
y = y - ym;

% summations for CCW boundary
xp = x( [2:end 1] );
yp = y( [2:end 1] );
a = x.*yp - xp.*y;

A = sum( a ) /2;
xc = sum( (x+xp).*a  ) /6/A;
yc = sum( (y+yp).*a  ) /6/A;
Ixx = sum( (y.*y +y.*yp + yp.*yp).*a  ) /12;
Iyy = sum( (x.*x +x.*xp + xp.*xp).*a  ) /12;
Ixy = sum( (x.*yp +2*x.*y +2*xp.*yp + xp.*y).*a  ) /24;

dx = xp - x;
dy = yp - y;
P = sum( sqrt( dx.*dx +dy.*dy ) );

% check for CCW versus CW boundary
if A < 0,
  A = -A;
  Ixx = -Ixx;
  Iyy = -Iyy;
  Ixy = -Ixy;
end

% centroidal moments
Iuu = Ixx - A*yc*yc;
Ivv = Iyy - A*xc*xc;
Iuv = Ixy - A*xc*yc;
J = Iuu + Ivv;
%
% replace mean of vertices
x_cen = xc + xm;
```

```
y_cen = yc + ym;
Ixx = Iuu + A*y_cen*y_cen;
Iyy = Ivv + A*x_cen*x_cen;
Ixy = Iuv + A*x_cen*y_cen;

% principal moments and orientation
I = [ Iuu  Iuv ;
     Iuv   Ivv ];
[ eig_vec, eig_val ] = eig(I);
I1 = eig_val(1,1);
I2 = eig_val(2,2);

ang2 = atan2( eig_vec(2,1), eig_vec(1,1) );
ang1 = atan2( eig_vec(2,2), eig_vec(1,2) );

ang1 = rad2deg(ang1+(ang1 < 0)*pi);
ang2 = rad2deg(ang2+(ang2 < 0)*pi);
% return values
geom = [ A  x_cen  y_cen  P ];
iner = [ Ixx  Iyy  Ixy  Iuu  Ivv  Iuv ];
cpmo = [ I2  ang2  I1  ang1  J ];

% bottom of polygeom
```

Appendix A.4 MATLAB Function "FindAngle"

```
%finds position of point on a curve, closest to specified
angle corresponding to principal moment angles
function Index = FindAngle(angle,princangle)


for i = 1:length(angle)
    anglediff(i) = abs(angle(i)-princangle);
end

[M,I] = min(anglediff);
Index = I;
```

Appendix B Average Data at Each Axis Angle

Appendix B Table 1- Average values for each category through all planes at 5° in the YZ Direction. (Mean ± SD)

Plane	Cross-Sectional Area (mm^2)	1st Principal 2nd Moment (mm^4)	2nd Principal 2nd Moment (mm^4)	Average Major Length (mm)	Average Minor Length (mm)	Maj/Min Axis Length Ratio	Average Major Axis Angle (deg.)
1	39.1 ± 16.7	313.4 ± 202.2	81.2 ± 123.5	10.5 ± 1.1	4.2 ± 1.1	2.6 ± 0.5	41.7 ± 14.0
2	34.7 ± 17.9	239.4 ± 221.6	70.4 ± 121.1	9.6 ± 1.1	4.2 ± 1.1	2.4 ± 0.5	40.2 ± 15.2
3	34.4 ± 18.3	214.9 ± 237.8	75.1 ± 121.6	8.9 ± 1.3	4.5 ± 1.0	2.0 ± 0.4	38.4 ± 18.4
4	36.6 ± 18.5	226.3 ± 255.0	89.5 ± 130.5	8.7 ±1.6	4.7 ± 1.0	1.9 ± 0.5	39.7 ± 25.1
5	45.3 ± 18.7	317.6 ± 282.5	134.1 ± 150.7	9.2 ± 1.6	5.4 ± 1.1	1.8 ± 0.5	43.2 ± 41.1

Appendix B Table 2- Average values for each category through all planes at 5° in the XY Direction. (Mean ± SD)

Plane	Cross-Sectional Area (mm^2)	1st Principal 2nd Moment (mm^4)	2nd Principal 2nd Moment (mm^4)	Average Major Length (mm)	Average Minor Length (mm)	Maj/Min Axis Lentgh Ratio	Average Major Axis Angle (deg.)
1	33.5 ± 5.3	231.3 ± 61.4	41.3 ± 15.7	10.3 ± 1.1	4.1 ± 0.6	2.6 ± 0.5	36.2 ± 8.7
2	29.2 ± 3.9	167.9 ± 51.7	31.7 ± 9.9	9.3 ± 1.0	4.0 ± 0.6	2.4 ± 0.5	34.4 ± 10.5
3	28.8 ± 3.9	140.7 ± 52.0	36.0 ±11.6	8.6 ± 1.0	4.3 ± 0.7	2.0 ± 0.4	32.2 ± 14.7
4	30.4 ± 4.3	144.0 ± 54.6	45.8 ± 19.2	8.3 ±1.2	4.4 ± 0.7	1.9 ± 0.5	33.4 ± 23.4
5	38.5± 8.4	220.9 ± 1110.4	80.4 ± 37.4	8.8 ± 1.4	5.0 ± 1.0	1.8 ± 0.5	37.1 ± 41.6

Appendix B Table 3– Average values for each category through all planes at 10° in the YZ Direction. (Mean ± SD)

Plane	Cross-Sectional Area (mm^2)	1st Principal 2nd Moment (mm^4)	2nd Principal 2nd Moment (mm^4)	Average Major Length (mm)	Average Minor Length (mm)	Maj/Min Axis Lentgh Ratio	Average Major Axis Angle (deg.)
1	39.2 ± 16.6	324.4 ± 210.8	79.2 ± 119.7	10.6 ± 1.2	4.2 ±1.1	2.6 ± 0.5	41.6 ±
2	34.5 ± 17.3	240.0 ± 219.6	67.7 ± 113.1	9.6 ± 1.2	4.2 ± 1.1	2.4 ± 0.5	40.0 ± 15.0
3	34.2 ± 17.5	210.8 ± 225.4	71.8 ± 109.9	8.9 ± 1.3	4.5 ± 1.0	2.0 ± 0.4	38.6 ± 18.3
4	37.2 ± 17.3	222.7 ± 235.3	89.0 ± 112.4	8.6 ± 1.5	4.9 ± 1.0	1.8 ± 0.3	40.2 ± 25.6
5	47.4 ± 17.6	326.1 ±259.8	142.8 ± 128.2	9.3 ± 1.5	5.7 ± 0.8	1.6 ± 0.2	43.7 ± 42.3

Appendix B Table 4– Average values for each category through all planes at 10° in the XY Direction. (Mean ± SD)

Plane	Cross-Sectional Area (mm^2)	1st Principal 2nd Moment (mm^4)	2nd Principal 2nd Moment (mm^4)	Average Major Length (mm)	Average Minor Length (mm)	Maj/Min Axis Lentgh Ratio	Average Major Axis Angle (deg.)
1	33.4 ± 5.3	229.6 ± 61.2	41.6 ± 16.2	10.2 ± 1.1	4.1 ± 0.6	2.6 ± 0.5	35.5 ±9.2
2	29.4 ± 3.7	166.9 ± 51.2	32.6 ± 9.7	9.3 ± 0.9	4.0 ± 0.6	2.4 ± 0.4	33.4 ± 11.2
3	29.0± 3.9	141.0 ± 51.6	36.9 ± 12.2	8.6 ± 1.0	4.3 ± 0.7	2.0 ± 0.4	31.5 ± 15.6
4	31.2 ± 4.9	146.6 ± 54.4	49.5 ± 20.6	8.3 ± 1.1	4.5 ± 0.6	1.8 ± 0.3	32.3 ± 24.9
5	41.1 ± 9.2	235.0 ± 123.8	88.6 ± 40.0	8.9 ± 1.4	5.1 ± 0.9	1.8 ± 0.2	35.3 ± 41.8

Appendix B Table 5– Average values for each category through all planes at 15° in the YZ Direction. (Mean ± SD)

Plane	Cross-Sectional Area (mm^2)	1st Principal 2nd Moment (mm^4)	2nd Principal 2nd Moment (mm^4)	Average Major Length (mm)	Average Minor Length (mm)	Maj/Min Axis Lentgh Ratio	Average Major Axis Angle (deg.)
1	39.1 ± 16.6	335.5 ± 222.2	76.3 ± 115.8	10.7 ± 1.2	4.1 ± 1.1	2.7 ± 0.5	42.1 ± 13.8
2	34.8 ± 17.2	248.9 ± 226.2	64.5 ± 110.4	9.7 ± 1.3	4.2 ± 1.1	2.4 ± 0.6	39.7 ± 14.8
3	34.4 ± 17.1	213.9 ± 223.5	70.8 ± 104.6	8.9 ± 1.4	4.5 ± 1.1	2.0 ± 0.4	38.7 ± 18.1
4	37.9 ± 16.7	225.6 ± 229.0	90.5 ± 105.5	8.6 ± 1.5	5.0 ± 1.0	1.8 ± 0.3	40.9 ± 26.0
5	49.3 ± 17.6	341.2 ± 258.4	155.5 ± 126.9	9.4 ± 1.4	6.0 ± 0.9	1.6 ± 0.2	44.0 ± 43.5

Appendix B Table 6– Average values for each category through all planes at 15° in the XY Direction. (Mean ± SD)

Plane	Cross-Sectional Area (mm^2)	1st Principal 2nd Moment (mm^4)	2nd Principal 2nd Moment (mm^4)	Average Major Length (mm)	Average Minor Length (mm)	Maj/Min Axis Lentgh Ratio	Average Major Axis Angle (deg.)
1	34.1 ± 5.7	228.1 ± 61.9	45.3 ± 18.4	10.2 ± 1.0	4.3 ± 0.7	2.4 ± 0.5	34.4 ± 10.2
2	30.3 ± 3.9	171.6 ± 51.4	36.3 ± 12.2	9.3 ± 0.9	4.2 ± 0.7	2.3 ± 0.5	32.2 ± 12.4
3	30.1 ± 3.8	147.5 ± 50.2	41.3 ± 14.0	8.6 ± 0.9	4.5 ± 0.7	2.0 ± 0.4	30.4 ± 16.4
4	31.9 ± 4.8	151.0 ± 52.8	52.3 ± 21.3	8.3 ± 1.1	4.6 ± 0.7	1.8 ± 0.3	30.9 ±25.7
5	39.5 ± 8.5	223.0 ± 113.1	87.7 ± 37.8	98.8 ± 1.4	5.2 ± 1.0	1.7 ± 0.3	32.7 ± 40.8

Appendix B Table 7– Average values for each category through all planes at 20° in the YZ Direction. (Mean ± SD)

Plane	Cross-Sectional Area (mm^2)	1st Principal 2nd Moment (mm^4)	2nd Principal 2nd Moment (mm^4)	Average Major Length (mm)	Average Minor Length (mm)	Maj/Min Axis Lentgh Ratio	Average Major Axis Angle (deg.)
1	39.7 ± 16.8	357.9 ± 235.6	75.6 ± 114.9	11.0 ± 1.3	4.1 ± 1.1	2.8 ± 0.6	41.6 ± 12.9
2	35.4 ± 17.2	263.2 ± 237.6	67.6 ± 108.4	9.9 ± 1.4	4.2 ± 1.2	2.5 ± 0.6	38.9 ± 14.1
3	34.9 ± 17.1	222.8 ± 229.7	71.7 ± 103.3	9.1 ± 1.4	4.6 ± 1.1	2.1 ± 0.5	38.2 ± 17.3
4	38.9 ± 16.4	232.8 ± 225.3	95.0 ± 103.4	8.7 ± 1.5	5.1 ± 1.1	1.7 ± 0.3	40.7 ± 26.2
5	51.9 ± 17.8	365.7 ± 258.6	173.1 ± 128.0	9.6 ± 1.3	6.2 ± 1.0	1.5 ± 0.2	43.5 ± 44.4

Appendix B Table 8– Average values for each category through all planes at 20° in the YZ Direction. (Mean ± SD)

Plane	Cross-Sectional Area (mm^2)	1st Principal 2nd Moment (mm^4)	2nd Principal 2nd Moment (mm^4)	Average Major Length (mm)	Average Minor Length (mm)	Maj/Min Axis Lentgh Ratio	Average Major Axis Angle (deg.)
1	34.7 ± 5.8	231.3 ± 64.0	48.4 ± 21.0	10.1 ± 1.0	4.4 ± 0.8	2.4 ± 0.5	33.9 ± 11.2
2	31.3 ± 4.1	177.3 ± 52.6	40.2 ± 14.3	9.3 ± 1.0	4.4 ± 0.7	2.2 ± 0.5	31.6 ± 13.4
3	31.2 ± 3.9	154.6 ± 50.0	45.4 ± 16.0	8.7 ± 0.9	4.6 ± 0.7	1.9 ± 0.4	30.1 ± 17.5
4	32.8 ± 4.9	157.3 ± 52.7	46.0 ± 22.3	8.4 ± 1.0	4.7 ± 0.7	1.8 ± 0.3	30.2 ± 26.8
5	39.7 ± 7.9	220.4 ± 100.5	89.5 ± 36.4	8.7 ± 1.4	5.3 ± 1.0	1.7 ± 0.3	31.3 ± 39.9

Appendix B Table 9– Average major and minor axis properties at 0° based on 2nd moment and PCA. (Mean ± SD)

Plane	Average Major Length (mm)		Average Minor Length (mm)		Maj/Min Axis Lentgh Ratio		Average Major Axis Angle (deg.)	
	2nd Moment	PCA	2nd Moment	PCA	2nd Moment	PCA	2nd Moment	PCA
1	10.6 ± 1.2	10.6 ± 1.1	4.3 ± 1.1	4.3 ± 1.1	2.5 ± 0.5	2.5 ± 0.5	41.1 ± 13.4	42.0 ± 16.1
2	9.6 ± 1.2	9.6 ± 1.2	4.3 ± 1.2	4.2 ± 1.1	2.4 ± 0.5	2.4 ± 0.5	39.7 ± 14.5	40.1 ± 15.6
3	9.0 ± 1.4	9.0 ± 1.4	4.6 ± 1.1	4.6 ± 1.1	2.0 ± 0.4	2.0 ± 0.4	37.6 ± 17.3	37.4 ± 17.2
4	8.7 ± 1.6	8.8 ± 1.7	4.8 ± 1.1	4.8 ± 1.1	1.9 ± 0.3	1.9 ± 0.4	38.5 ± 23.0	37.4 ± 22.3
5	9.2 ± 1.7	9.3 ± 1.8	5.4 ± 1.1	5.5 ± 1.2	1.7 ± 0.3	1.7 ± 0.4	41.7 ± 39.2	41.1 ± 40.6

Appendix C Cross-sectional Property Raw Data

Appendix C Table 1 – Cross-sectional area data at 0° (mm^2)

	Sample 1	Sample 2	Sample 3	Sample 4	Sample 5	Sample 6	Sample 7	Sample 8	Sample 9
1	39.1	35.3	28.7	35.7	34.7	40.5	30.7	23.3	86.3
2	32.6	33.9	26.0	28.6	28.5	32.9	27.2	22.4	87.0
3	32.8	34.6	25.4	28.1	28.5	30.1	25.1	23.5	87.9
4	37.2	36.4	27.6	30.4	30.2	29.4	27.5	24.7	89.2
5	52.9	41.4	36.0	39.0	38.8	39.5	31.6	29.6	90.5

Appendix C Table 2 – 1st principal 2nd moment data at 0° (mm^4)

	Sample 1	Sample 2	Sample 3	Sample 4	Sample 5	Sample 6	Sample 7	Sample 8	Sample 9
1	271.2	285.6	139.6	266.4	270.0	324.2	229.6	125.9	906.3
2	183.7	263.2	93.0	185.4	166.3	190.0	161.9	104.5	928.9
3	147.3	257.7	83.7	159.8	130.0	134.4	117.8	95.1	956.5
4	156.0	267.0	88.3	164.4	122.5	125.5	123.3	97.1	992.7
5	396.7	335.8	148.9	221.5	161.5	187.3	151.8	136.5	1034.3

Appendix C Table 3 – 2nd principal 2nd moment data at 0° (mm^4)

	Sample 1	Sample 2	Sample 3	Sample 4	Sample 5	Sample 6	Sample 7	Sample 8	Sample 9
1	62.3	42.5	33.8	43.4	35.7	58.4	27.0	16.1	471.5
2	40.1	36.7	34.6	25.6	25.7	43.0	22.6	16.4	479.2
3	50.9	40.4	35.8	27.8	32.9	43.3	21.8	21.8	490.0
4	80.3	49.4	51.3	35.1	44.0	43.6	30.8	28.0	509.0
5	133.5	67.2	94.2	69.4	90.1	91.7	48.1	42.4	528.4

Appendix C Table 4 – Major axis angle data at 0° (deg.)

	Sample 1	Sample 2	Sample 3	Sample 4	Sample 5	Sample 6	Sample 7	Sample 8	Sample 9
1	31.5	23.2	49.1	36.0	45.3	35.7	41.3	37.4	70.8
2	21.0	24.3	47.5	40.2	45.5	30.2	42.3	36.8	69.6
3	9.5	24.1	58.5	34.6	38.1	32.6	38.9	34.1	68.1
4	-2.8	23.8	75.1	27.7	41.9	43.4	38.4	32.4	66.6
5	-13.8	22.2	125.7	19.8	31.0	59.9	41.8	24.1	65.0

Appendix C Table 5 – Major axis length data at 0° (mm)

	Sample 1	Sample 2	Sample 3	Sample 4	Sample 5	Sample 6	Sample 7	Sample 8	Sample 9
1	10.5	11.3	8.5	10.9	11.2	11.9	10.4	8.8	11.5
2	9.3	11.0	7.8	9.8	9.6	9.7	9.4	8.2	11.6
3	8.4	10.8	7.7	9.1	8.4	8.6	8.6	7.6	11.8
4	7.9	10.7	7.1	9.0	7.9	7.9	8.4	7.3	12.0
5	10.5	11.1	7.1	9.4	8.2	8.2	7.9	8.1	12.3

Appendix C Table 6 – Minor axis length data at 0° (mm)

	Sample 1	Sample 2	Sample 3	Sample 4	Sample 5	Sample 6	Sample 7	Sample 8	Sample 9
1	4.7	3.7	4.3	4.1	4.0	4.7	3.4	3.2	6.9
2	4.4	3.7	4.6	3.5	3.8	4.5	3.5	3.2	7.0
3	4.9	4.0	5.3	3.7	4.2	4.7	3.6	3.7	7.1
4	5.5	4.2	4.4	4.1	4.8	4.4	4.1	3.9	7.3
5	6.3	4.4	4.8	5.6	6.1	5.1	4.5	4.2	7.5

Appendix C Table 7 – Major-to-Minor axis length ratio data at 0°

	Sample 1	Sample 2	Sample 3	Sample 4	Sample 5	Sample 6	Sample 7	Sample 8	Sample 9
1	2.3	3.1	2.0	2.7	2.8	2.5	3.1	2.8	1.7
2	2.1	3.0	1.7	2.8	2.5	2.1	2.7	2.5	1.7
3	1.7	2.7	1.4	2.5	2.0	1.8	2.4	2.1	1.7
4	1.4	2.6	1.6	2.2	1.7	1.8	2.0	1.9	1.6
5	1.7	2.5	1.5	1.7	1.3	1.6	1.8	1.9	1.6

Appendix C Table 8 – PCA major axis angle data at 0° (deg.)

	Sample1	Sample2	Sample3	Sample4	Sample5	Sample6	Sample7	Sample8	Sample9
1	30.4	23.1	51.5	34.8	45.4	36.1	41.4	36.5	78.9
2	20.9	24.6	47.9	39.4	45.8	30.8	42.1	35.4	73.6
3	9.7	24.1	56.8	34.6	39.2	32.2	39.2	32.1	68.6
4	-2.7	23.1	72.9	27.8	42.0	40.5	38.6	29.6	64.3
5	-12.9	21.3	131.8	18.7	31.3	59.4	36.6	23.3	60.6

Appendix C Table 9 – PCA major axis length data at 0° (mm)

	Sample1	Sample2	Sample3	Sample4	Sample5	Sample6	Sample7	Sample8	Sample9
1	10.6	11.3	8.6	10.9	11.2	11.9	10.4	8.9	11.3
2	9.2	11.0	7.8	9.8	9.6	9.8	9.4	8.2	11.5
3	8.4	10.8	7.7	9.1	8.5	8.6	8.6	7.7	11.8
4	7.9	10.8	7.3	9.0	7.9	7.9	8.4	7.4	12.2
5	10.5	11.1	7.2	9.4	8.2	8.2	8.1	8.2	12.6

Appendix C Table 10 – PCA minor axis length data at 0° (mm)

	Sample1	Sample2	Sample3	Sample4	Sample5	Sample6	Sample7	Sample8	Sample9
1	4.7	3.7	4.3	4.1	4.0	4.7	3.4	3.2	7.1
2	4.4	3.7	4.6	3.5	3.8	4.5	3.5	3.2	6.9
3	4.9	4.0	5.3	3.7	4.3	4.7	3.6	3.6	7.1
4	5.5	4.2	4.5	4.1	4.8	4.5	4.1	3.9	7.5
5	6.3	4.4	5.4	5.6	6.1	5.1	4.4	4.2	8.1

Appendix C Table 11 – PCA Major-to-Minor axis length ratio data at 0°

	Sample1	Sample2	Sample3	Sample4	Sample5	Sample6	Sample7	Sample8	Sample9
1	2.3	3.1	2.0	2.7	2.8	2.5	3.1	2.8	1.6
2	2.1	3.0	1.7	2.8	2.5	2.2	2.7	2.6	1.7
3	1.7	2.7	1.5	2.5	2.0	1.8	2.4	2.1	1.7
4	1.4	2.6	1.6	2.2	1.7	1.7	2.0	1.9	1.6
5	1.7	2.5	1.3	1.7	1.3	1.6	1.8	1.9	1.6

Appendix C Table 12 – Cross-sectional area data at 5° in the YZ plane (mm^2)

	Sample 1	Sample 2	Sample 3	Sample 4	Sample 5	Sample 6	Sample 7	Sample 8	Sample 9
1	39.7	36.7	29.3	35.2	36.3	38.5	31.8	23.1	81.6
2	32.0	33.6	25.9	28.5	28.9	32.1	27.2	22.3	81.3
3	32.6	34.6	25.4	27.9	28.6	29.3	25.4	23.3	82.2
4	38.7	33.6	28.4	30.8	30.1	29.9	27.8	24.8	84.9
5	58.4	36.7	38.4	40.2	39.6	41.4	32.3	30.0	90.4

Appendix C Table 13 - 1st principal 2nd moment data at 5° in the YZ plane (mm^4)

	Sample 1	Sample 2	Sample 3	Sample 4	Sample 5	Sample 6	Sample 7	Sample 8	Sample 9
1	279.5	308.4	148.6	278.0	292.9	323.3	245.6	124.5	820.0
2	172.2	260.1	93.7	190.2	176.3	178.9	163.5	104.1	816.0
3	136.5	249.3	83.9	157.4	131.1	125.7	120.7	93.0	836.2
4	160.9	260.1	93.6	162.2	120.3	125.8	124.7	96.1	892.8
5	465.5	308.4	178.4	221.6	164.4	206.9	156.9	135.9	1020.1

Appendix C Table 14 - 2nd principal 2nd moment data at 5° in the YZ plane (mm^4)

	Sample 1	Sample 2	Sample 3	Sample 4	Sample 5	Sample 6	Sample 7	Sample 8	Sample 9
1	63.5	47.7	33.9	39.7	41.1	51.9	28.7	16.0	408.5
2	39.2	36.1	34.1	24.9	25.8	41.7	22.8	16.1	392.7
3	53.4	41.8	35.4	27.9	32.9	41.7	22.7	21.6	398.3
4	91.1	36.1	54.7	37.3	44.3	46.6	32.0	29.1	433.9
5	166.8	47.7	100.0	78.6	95.2	99.9	50.7	44.5	523.0

Appendix C Table 15 – Major axis angle data at 5° in the YZ plane (deg.)

	Sample 1	Sample 2	Sample 3	Sample 4	Sample 5	Sample 6	Sample 7	Sample 8	Sample 9
1	32.2	23.3	51.1	37.3	43.8	36.1	40.8	37.3	73.0
2	20.7	24.4	47.9	41.5	45.6	30.6	42.2	36.8	72.3
3	8.6	23.8	59.5	35.2	37.8	35.2	38.3	34.6	72.2
4	-5.1	24.4	77.9	27.4	42.2	45.8	39.7	32.5	72.5
5	-13.9	23.3	130.4	17.8	30.3	62.2	42.8	24.7	70.6

Appendix C Table 16 - Major axis length data at 5° in the YZ plane (mm)

	Sample 1	Sample 2	Sample 3	Sample 4	Sample 5	Sample 6	Sample 7	Sample 8	Sample 9
1	10.4	11.4	8.6	11.1	11.4	11.7	10.6	8.8	11.0
2	9.1	11.0	7.9	10.0	9.9	9.5	9.3	8.2	11.4
3	8.2	10.6	7.7	9.1	8.4	8.4	8.6	7.5	11.5
4	7.8	11.0	7.1	9.0	7.9	7.8	8.4	7.3	11.7
5	10.7	10.3	7.6	9.3	8.2	8.5	8.0	8.0	12.3

Appendix C Table 17 - Minor axis length data at 5° in the YZ plane (mm)

	Sample 1	Sample 2	Sample 3	Sample 4	Sample 5	Sample 6	Sample 7	Sample 8	Sample 9
1	4.7	3.7	4.2	3.9	4.0	4.2	3.5	3.2	6.8
2	4.4	3.7	4.6	3.3	3.9	4.5	3.5	3.2	6.8
3	5.0	4.0	5.3	3.6	4.2	4.6	3.6	3.7	6.8
4	5.9	3.6	4.4	4.3	4.8	4.4	4.2	3.9	6.8
5	6.4	3.4	5.4	5.8	6.2	5.4	4.6	4.4	6.9

Appendix C Table 18 - Major-to-Minor axis length ratio data at 5° in the YZ plane

	Sample 1	Sample 2	Sample 3	Sample 4	Sample 5	Sample 6	Sample 7	Sample 8	Sample 9
1	2.2	3.1	2.0	2.9	2.8	2.8	3.1	2.7	1.6
2	2.0	3.0	1.7	3.0	2.5	2.1	2.7	2.6	1.7
3	1.6	2.7	1.5	2.5	2.0	1.8	2.4	2.0	1.7
4	1.3	3.1	1.6	2.1	1.6	1.7	2.0	1.9	1.7
5	1.7	3.0	1.4	1.6	1.3	1.6	1.7	1.8	1.8

Appendix C Table 19 - Cross-sectional area data at 10° in the YZ plane (mm^2)

	Sample 1	Sample 2	Sample 3	Sample 4	Sample 5	Sample 6	Sample 7	Sample 8	Sample 9
1	39.0	37.8	29.6	34.6	37.6	37.3	32.5	22.8	81.2
2	31.4	33.6	26.0	28.7	29.6	31.5	27.4	22.4	79.9
3	32.9	34.5	25.6	28.0	28.8	28.7	26.1	23.3	79.8
4	40.5	37.0	29.2	31.7	30.5	30.7	28.5	25.2	81.7
5	63.6	46.1	40.3	41.9	41.1	43.7	33.3	30.0	87.0

Appendix C Table 20 - 1st principal 2nd moment data at 10° in the YZ plane (mm^4)

	Sample 1	Sample 2	Sample 3	Sample 4	Sample 5	Sample 6	Sample 7	Sample 8	Sample 9
1	271.2	336.2	155.7	288.3	312.5	325.1	258.0	121.7	851.0
2	158.1	265.7	95.7	201.1	187.9	169.4	167.0	105.2	809.9
3	131.8	248.2	86.1	158.1	133.4	120.9	126.6	93.1	798.6
4	171.6	253.9	99.2	165.6	121.2	128.4	131.0	96.6	837.0
5	521.7	335.7	198.3	230.7	175.5	230.0	166.6	132.7	943.7

Appendix C Table 21 - 2nd principal 2nd moment data at 10° in the YZ plane (mm^4)

	Sample 1	Sample 2	Sample 3	Sample 4	Sample 5	Sample 6	Sample 7	Sample 8	Sample 9
1	59.1	47.7	33.4	36.5	45.5	48.5	29.6	15.6	396.7
2	39.5	36.1	34.0	24.5	26.2	41.2	23.2	16.4	368.5
3	56.8	42.3	35.5	28.3	33.1	40.3	24.3	21.8	363.6
4	102.1	55.8	57.4	41.3	45.9	50.2	34.3	30.3	383.3
5	207.7	105.7	105.6	89.9	104.1	110.7	54.3	45.3	462.0

Appendix C Table 22 – Major axis angle data at 10° in the YZ plane (deg.)

	Sample 1	Sample 2	Sample 3	Sample 4	Sample 5	Sample 6	Sample 7	Sample 8	Sample 9
1	31.5	24.2	52.2	38.5	43.3	36.7	40.2	37.1	70.7
2	20.0	24.3	48.1	42.2	45.4	31.0	41.8	36.5	70.9
3	9.1	23.5	59.5	35.4	37.4	37.7	37.7	34.9	72.2
4	-4.7	23.8	79.3	27.1	42.0	47.8	40.6	32.3	73.9
5	-15.2	25.2	130.7	14.5	28.2	64.2	43.3	25.8	76.3

Appendix C Table 23 - Major axis length data at 10° in the YZ plane (mm)

	Sample 1	Sample 2	Sample 3	Sample 4	Sample 5	Sample 6	Sample 7	Sample 8	Sample 9
1	10.1	11.6	8.7	11.2	11.6	11.6	10.7	8.7	11.2
2	8.7	11.1	7.9	10.2	10.1	9.4	9.4	8.2	11.5
3	7.9	10.5	7.7	9.1	8.5	8.3	8.7	7.6	11.5
4	7.8	10.4	7.1	9.0	7.9	7.7	8.5	7.3	11.7
5	10.8	11.0	8.0	9.3	8.3	8.6	8.1	7.9	11.9

Appendix C Table 24 - Minor axis length data at 10° in the YZ plane (mm)

	Sample 1	Sample 2	Sample 3	Sample 4	Sample 5	Sample 6	Sample 7	Sample 8	Sample 9
1	4.7	3.7	4.1	3.7	4.2	3.8	3.5	3.2	6.8
2	4.5	3.7	4.6	3.2	4.0	4.5	3.5	3.2	6.8
3	5.2	4.0	5.2	3.6	4.2	4.5	3.6	3.7	6.8
4	6.3	4.4	4.3	4.5	4.8	4.4	4.2	3.9	6.9
5	6.7	5.2	5.6	5.9	6.3	5.6	4.8	4.5	6.9

Appendix C Table 25 - Major-to-Minor axis length ratio data at 10° in the YZ plane

	Sample 1	Sample 2	Sample 3	Sample 4	Sample 5	Sample 6	Sample 7	Sample 8	Sample 9
1	2.2	3.1	2.1	3.0	2.8	3.0	3.1	2.8	1.6
2	2.0	3.0	1.7	3.2	2.6	2.1	2.7	2.5	1.7
3	1.5	2.7	1.5	2.5	2.0	1.8	2.4	2.0	1.7
4	1.2	2.3	1.6	2.0	1.6	1.7	2.0	1.8	1.7
5	1.6	2.1	1.4	1.6	1.3	1.5	1.7	1.8	1.7

Appendix C Table 26 - Cross-sectional area data at 15° in the YZ plane (mm^2)

	Sample 1	Sample 2	Sample 3	Sample 4	Sample 5	Sample 6	Sample 7	Sample 8	Sample 9
1	38.7	39.6	30.1	34.6	34.8	35.9	34.2	22.8	81.4
2	31.4	34.3	26.3	29.2	30.3	31.3	28.0	22.7	79.7
3	33.5	34.8	26.0	28.4	28.9	28.5	26.7	23.5	79.1
4	42.2	37.4	30.0	33.1	31.3	31.1	29.5	25.7	80.6
5	68.5	47.0	42.0	44.0	43.1	47.6	34.6	30.3	86.9

Appendix C Table 27 - 1st principal 2nd moment data at 15° in the YZ plane (mm^4)

	Sample 1	Sample 2	Sample 3	Sample 4	Sample 5	Sample 6	Sample 7	Sample 8	Sample 9
1	276.7	383.6	165.3	305.0	288.8	306.7	283.6	120.4	889.8
2	152.8	285.2	99.2	217.0	197.8	165.3	178.8	110.2	833.3
3	133.9	254.8	89.7	163.0	135.8	121.4	134.7	95.7	795.8
4	183.0	256.6	104.8	172.8	125.4	127.7	139.0	98.6	822.5
5	570.1	329.1	213.8	246.8	190.5	268.3	179.2	132.6	940.1

Appendix C Table 28 - 2nd principal 2nd moment data at 15° in the YZ plane (mm^4)

	Sample 1	Sample 2	Sample 3	Sample 4	Sample 5	Sample 6	Sample 7	Sample 8	Sample 9
1	54.6	49.5	33.7	35.3	35.8	44.9	32.8	15.8	383.7
2	40.6	36.7	34.3	2.4	27.3	41.6	23.9	16.7	357.0
3	60.6	43.1	36.4	29.2	33.3	39.1	25.5	21.8	348.1
4	112.3	58.0	60.2	46.9	49.2	53.8	37.4	31.9	365.1
5	254.2	118.1	112.6	103.3	115.6	134.3	58.5	46.9	455.5

Appendix C Table 29 – Major axis angle data at 15° in the YZ plane (deg.)

	Sample 1	Sample 2	Sample 3	Sample 4	Sample 5	Sample 6	Sample 7	Sample 8	Sample 9
1	30.4	25.1	53.1	39.2	45.4	36.5	40.1	36.7	71.9
2	19.4	24.2	47.7	42.5	44.4	31.5	41.1	35.9	70.2
3	10.1	22.9	58.8	35.3	36.7	39.5	37.7	34.9	72.1
4	-3.3	23.4	79.9	26.8	41.1	50.9	41.0	31.8	76.2
5	-16.8	26.8	130.4	11.4	25.1	65.5	43.7	26.4	83.0

Appendix C Table 30 - Major axis length data at 15° in the YZ plane (mm)

	Sample 1	Sample 2	Sample 3	Sample 4	Sample 5	Sample 6	Sample 7	Sample 8	Sample 9
1	10.3	11.9	8.8	11.3	11.7	11.4	10.9	8.7	11.6
2	8.6	11.2	8.0	10.5	10.2	9.4	9.5	8.3	11.6
3	7.8	10.6	7.8	9.2	8.5	8.3	8.8	7.7	11.6
4	7.8	10.4	7.1	9.0	7.9	7.5	8.5	7.4	11.7
5	11.0	10.8	8.2	9.4	8.5	8.9	8.2	7.8	11.8

Appendix C Table 31 - Minor axis length data at 15° in the YZ plane (mm)

	Sample 1	Sample 2	Sample 3	Sample 4	Sample 5	Sample 6	Sample 7	Sample 8	Sample 9
1	4.5	3.7	3.9	3.6	4.0	3.7	3.6	3.2	6.8
2	4.5	3.6	4.5	3.2	4.0	4.4	3.4	3.2	6.9
3	5.3	3.9	5.2	3.6	4.2	4.4	3.6	3.7	6.9
4	6.5	4.5	4.4	4.8	4.9	4.4	4.3	4.0	6.9
5	7.1	5.6	5.9	6.1	6.5	6.0	4.9	4.6	7.1

Appendix C Table 32 - Major-to-Minor axis length ratio data at 15° in the YZ plane

	Sample 1	Sample 2	Sample 3	Sample 4	Sample 5	Sample 6	Sample 7	Sample 8	Sample 9
1	2.3	3.2	2.2	3.2	3.0	3.1	3.1	2.7	1.7
2	1.9	3.1	1.8	3.3	2.6	2.1	2.8	2.6	1.7
3	1.5	2.7	1.5	2.6	2.0	1.9	2.4	2.1	1.7
4	1.2	2.3	1.6	1.9	1.6	1.7	2.0	1.8	1.7
5	1.5	1.9	1.4	1.5	1.3	1.5	1.7	1.7	1.7

Appendix C Table 33 - Cross-sectional area data at 20° in the YZ plane (mm^2)

	Sample 1	Sample 2	Sample 3	Sample 4	Sample 5	Sample 6	Sample 7	Sample 8	Sample 9
1	38.2	42.7	30.9	34.7	34.1	35.3	36.1	22.8	82.1
2	31.6	35.6	26.9	29.7	31.3	31.0	28.7	23.3	80.3
3	34.6	35.3	26.8	29.0	29.3	28.6	27.5	23.9	79.4
4	44.4	38.2	31.3	34.7	32.4	31.9	30.9	26.5	80.4
5	75.7	48.5	44.9	46.7	45.6	51.7	37.0	30.8	86.3

Appendix C Table 34 - 1st principal 2nd moment data at 20° in the YZ plane (mm^4)

	Sample 1	Sample 2	Sample 3	Sample 4	Sample 5	Sample 6	Sample 7	Sample 8	Sample 9
1	280.5	465.1	177.4	334.1	290.2	297.4	324.8	121.1	930.6
2	150.0	322.1	105.0	235.0	212.8	162.0	192.8	117.5	872.0
3	140.8	269.5	94.8	171.4	140.4	125.2	143.1	100.2	819.9
4	201.5	267.6	111.9	181.9	132.0	130.5	148.8	103.2	817.7
5	656.6	337.3	240.4	268.9	212.7	303.7	205.9	135.4	930.3

Appendix C Table 35 - 2nd principal 2nd moment data at 20° in the YZ plane (mm^4)

	Sample 1	Sample 2	Sample 3	Sample 4	Sample 5	Sample 6	Sample 7	Sample 8	Sample 9
1	50.3	53.8	35.0	33.2	32.5	44.1	35.2	16.0	380.7
2	42.4	38.1	35.2	24.7	28.9	41.4	24.4	17.4	355.7
3	65.2	44.1	38.6	30.9	33.7	38.2	26.9	22.4	345.3
4	124.4	60.6	65.5	54.2	53.6	58.5	42.0	34.0	362.0
5	328.2	131.0	127.0	120.6	129.9	164.4	66.9	49.1	441.1

Appendix C Table 36 – Major axis angle data at 20° in the YZ plane (deg.)

	Sample 1	Sample 2	Sample 3	Sample 4	Sample 5	Sample 6	Sample 7	Sample 8	Sample 9
1	29.1	26.3	53.8	40.2	45.9	35.9	39.5	36.0	68.0
2	18.5	24.2	47.0	42.4	43.2	32.7	40.0	35.0	67.3
3	10.8	22.3	57.6	34.8	36.0	40.8	37.7	34.4	69.4
4	-3.1	22.8	80.3	25.8	39.7	54.1	41.3	30.8	74.8
5	-18.2	27.3	130.2	8.7	21.0	68.5	44.6	26.5	82.5

Appendix C Table 37 - Major axis length data at 20° in the YZ plane (mm)

	Sample 1	Sample 2	Sample 3	Sample 4	Sample 5	Sample 6	Sample 7	Sample 8	Sample 9
1	10.5	12.5	8.9	11.6	11.9	11.4	11.4	8.7	11.8
2	8.5	11.5	8.2	10.8	10.4	9.4	9.8	8.5	11.9
3	7.9	10.8	7.9	9.4	8.6	8.4	9.0	7.8	11.7
4	8.1	10.6	7.1	9.0	7.9	7.5	8.7	7.5	11.6
5	11.2	10.7	8.5	9.5	8.8	9.2	8.5	7.8	11.7

Appendix C Table 38 - Minor axis length data at 20° in the YZ plane (mm)

	Sample 1	Sample 2	Sample 3	Sample 4	Sample 5	Sample 6	Sample 7	Sample 8	Sample 9
1	4.4	3.7	3.8	3.4	3.9	3.6	3.6	3.2	6.9
2	4.6	3.5	4.5	3.1	4.0	4.4	3.4	3.2	7.0
3	5.4	3.9	5.2	3.6	4.2	4.4	3.7	3.8	7.0
4	6.8	4.5	4.4	5.1	5.1	4.5	4.4	4.0	7.0
5	7.7	5.8	6.2	6.3	6.6	6.5	5.1	4.7	7.2

Appendix C Table 39 - Major-to-Minor axis length ratio data at 20° in the YZ plane

	Sample 1	Sample 2	Sample 3	Sample 4	Sample 5	Sample 6	Sample 7	Sample 8	Sample 9
1	2.4	3.4	2.3	3.4	3.1	3.1	3.1	2.7	1.7
2	1.9	3.3	1.8	3.5	2.6	2.1	2.9	2.6	1.7
3	1.5	2.8	1.5	2.6	2.0	1.9	2.4	2.1	1.7
4	1.2	2.4	1.6	1.8	1.6	1.7	2.0	1.9	1.7
5	1.5	1.9	1.4	1.5	1.3	1.4	1.7	1.7	1.6

Appendix C Table 40 - Cross-sectional area data at 5° in the XY plane (mm^2)

	Sample 1	Sample 2	Sample 3	Sample 4	Sample 5	Sample 6	Sample 7	Sample 8
1	39.7	35.4	29.5	36.4	34.9	37.9	31.2	23.3
2	32.9	33.9	26.4	29.2	28.8	32.8	27.4	22.4
3	33.6	34.7	25.8	28.5	28.7	30.3	25.6	23.5
4	38.8	33.9	27.8	30.8	30.3	29.8	28.0	24.5
5	57.1	35.4	36.7	39.6	39.4	39.0	32.0	29.1

Appendix C Table 41 - 1st principal 2nd moment data at 5° in the XY plane (mm^4)

	Sample 1	Sample 2	Sample 3	Sample 4	Sample 5	Sample 6	Sample 7	Sample 8
1	260.6	284.6	146.1	270.3	261.1	267.9	236.7	123.0
2	178.5	260.0	94.9	188.7	171.6	183.0	162.4	103.8
3	145.9	254.2	86.0	160.6	130.5	132.6	120.9	94.9
4	167.0	260.0	89.5	165.7	121.2	126.6	126.2	96.1
5	466.0	284.6	160.5	227.0	161.7	180.4	156.2	130.9

Appendix C Table 42 – 2nd principal 2nd moment data at 5° in the XY plane (mm^4)

	Sample 1	Sample 2	Sample 3	Sample 4	Sample 5	Sample 6	Sample 7	Sample 8
1	67.5	43.6	36.1	45.6	39.2	54.9	27.8	16.4
2	42.6	37.0	36.4	27.6	26.0	44.2	23.3	16.5
3	56.3	41.5	37.2	29.3	33.4	45.4	23.2	21.9
4	89.0	37.0	52.7	36.7	44.8	46.0	32.8	27.7
5	153.0	43.6	97.9	72.5	95.6	89.8	49.9	41.1

Appendix C Table 43 – Major axis angle data at 5° in the XY plane (deg.)

	Sample 1	Sample 2	Sample 3	Sample 4	Sample 5	Sample 6	Sample 7	Sample 8
1	30.4	21.3	49.7	37.2	43.6	31.4	39.9	35.9
2	18.2	22.5	47.3	39.6	43.7	27.9	41.0	35.3
3	5.7	22.2	57.9	33.5	36.3	31.7	37.7	32.8
4	-8.8	22.5	75.1	26.2	40.2	42.3	38.4	31.4
5	-17.2	21.3	125.5	17.3	28.3	57.9	40.5	23.3

Appendix C Table 44 – Major axis length data at 5° in the XY plane (deg.)

	Sample 1	Sample 2	Sample 3	Sample 4	Sample 5	Sample 6	Sample 7	Sample 8
1	10.2	11.2	8.5	10.8	11.1	11.4	10.5	8.7
2	9.1	10.9	7.9	9.8	9.7	9.5	9.3	8.2
3	8.4	10.7	7.7	9.1	8.4	8.5	8.6	7.6
4	8.0	10.9	7.2	9.0	7.9	7.8	8.4	7.3
5	10.9	10.8	7.2	9.4	8.1	8.2	8.0	8.0

Appendix C Table 45 - Minor axis length data at 5° in the XY plane (mm)

	Sample 1	Sample 2	Sample 3	Sample 4	Sample 5	Sample 6	Sample 7	Sample 8
1	4.8	3.7	4.4	4.2	4.1	4.8	3.4	3.3
2	4.6	3.7	4.7	3.6	3.8	4.6	3.5	3.2
3	5.1	4.0	5.4	3.7	4.3	4.8	3.6	3.7
4	5.8	3.6	4.4	4.2	4.8	4.4	4.2	3.9
5	6.3	3.3	4.6	5.6	6.2	5.1	4.5	4.2

Appendix C Table 46 - Major-to-Minor axis length ratio data at 5° in the XY plane

	Sample 1	Sample 2	Sample 3	Sample 4	Sample 5	Sample 6	Sample 7	Sample 8
1	2.1	3.0	1.9	2.6	2.7	2.4	3.1	2.7
2	2.0	2.9	1.7	2.8	2.5	2.1	2.7	2.5
3	1.6	2.7	1.4	2.4	2.0	1.8	2.4	2.1
4	1.4	3.1	1.6	2.2	1.6	1.8	2.0	1.9
5	1.7	3.3	1.6	1.7	1.3	1.6	1.8	1.9

Appendix C Table 47 - Cross-sectional area data at 10° in the XY plane (mm^2)

	Sample 1	Sample 2	Sample 3	Sample 4	Sample 5	Sample 6	Sample 7	Sample 8
1	40.0	35.4	29.9	37.8	34.9	34.9	31.4	23.1
2	33.5	34.1	27.1	30.1	29.3	30.6	27.7	22.6
3	34.5	34.7	26.4	29.0	29.0	28.0	26.6	23.8
4	40.2	36.2	28.0	31.6	30.4	30.0	28.8	24.7
5	59.7	39.9	36.2	40.9	39.8	42.8	32.4	29.2

Appendix C Table 48 - 1st principal 2nd moment data at 10° in the XY plane (mm^4)

	Sample 1	Sample 2	Sample 3	Sample 4	Sample 5	Sample 6	Sample 7	Sample 8
1	247.1	282.3	149.4	282.3	253.0	262.2	241.7	119.0
2	172.9	260.2	98.9	195.3	178.3	162.6	163.6	103.4
3	146.6	253.5	90.5	163.7	132.6	117.5	128.0	95.6
4	177.2	258.4	92.4	169.9	121.0	125.2	131.8	96.9
5	508.4	298.9	156.8	240.2	160.5	225.9	159.2	130.3

Appendix C Table 49 – 2nd principal 2nd moment data at 10° in the XY plane (mm^4)

	Sample 1	Sample 2	Sample 3	Sample 4	Sample 5	Sample 6	Sample 7	Sample 8
1	71.9	43.2	38.2	50.7	41.9	42.6	27.9	16.5
2	46.9	38.0	38.9	30.2	26.8	38.5	24.2	17.1
3	62.3	41.9	39.3	31.2	34.5	37.3	25.5	22.9
4	96.4	50.1	53.2	39.8	45.8	46.8	35.4	28.2
5	169.1	65.6	98.0	78.0	100.7	104.1	51.4	41.7

Appendix C Table 50 – Major axis angle data at 10° in the XY plane (deg.)

	Sample 1	Sample 2	Sample 3	Sample 4	Sample 5	Sample 6	Sample 7	Sample 8
1	28.9	19.7	50.2	38.2	42.4	31.2	38.7	34.7
2	15.3	20.7	47.9	39.2	42.1	28.2	40.0	33.8
3	2.6	20.6	57.9	32.7	34.8	34.9	37.1	31.7
4	-14.1	20.5	74.3	25.2	38.7	44.7	38.9	30.6
5	-22.8	20.4	121.0	14.1	27.6	59.6	40.0	22.5

Appendix C Table 51 – Major axis length data at 10° in the XY plane (deg.)

	Sample 1	Sample 2	Sample 3	Sample 4	Sample 5	Sample 6	Sample 7	Sample 8
1	9.8	11.2	8.6	10.8	11.0	11.3	10.5	8.6
2	8.9	10.9	8.0	9.8	9.8	9.4	9.3	8.2
3	8.3	10.6	7.8	9.1	8.5	8.2	8.6	7.6
4	8.2	10.5	7.3	9.0	7.9	7.7	8.5	7.3
5	11.1	10.8	7.2	9.4	7.9	8.6	8.0	8.0

Appendix C Table 52 - Minor axis length data at 10° in the XY plane (mm)

	Sample 1	Sample 2	Sample 3	Sample 4	Sample 5	Sample 6	Sample 7	Sample 8
1	5.0	3.7	4.6	4.4	4.2	4.1	3.3	3.3
2	4.7	3.8	4.9	3.6	3.9	4.4	3.6	3.3
3	5.3	4.0	5.5	3.8	4.3	4.4	3.7	3.7
4	6.0	4.2	4.4	4.3	4.9	4.3	4.3	3.9
5	6.3	4.4	4.3	5.6	6.3	5.5	4.6	4.2

Appendix C Table 53 - Major-to-Minor axis length ratio data at 10° in the XY plane

	Sample 1	Sample 2	Sample 3	Sample 4	Sample 5	Sample 6	Sample 7	Sample 8
1	1.9	3.0	1.9	2.5	2.6	2.7	3.2	2.6
2	1.9	2.9	1.6	2.7	2.5	2.1	2.6	2.5
3	1.6	2.7	1.4	2.4	2.0	1.9	2.3	2.0
4	1.4	2.5	1.7	2.1	1.6	1.8	2.0	1.9
5	1.8	2.5	1.7	1.7	1.3	1.6	1.7	1.9

Appendix C Table 54 - Cross-sectional area data at 15° in the XY plane (mm^2)

	Sample 1	Sample 2	Sample 3	Sample 4	Sample 5	Sample 6	Sample 7	Sample 8
1	40.7	35.4	30.3	39.1	35.3	36.8	31.6	23.3
2	34.5	34.5	28.0	31.3	30.0	33.2	28.2	23.0
3	35.7	35.0	27.3	29.9	29.6	31.2	28.0	24.3
4	40.9	36.2	28.6	32.5	30.8	31.2	30.0	25.0
5	58.1	38.3	35.6	41.1	40.8	39.5	33.4	29.3

Appendix C Table 55 - 1st principal 2nd moment data at 15° in the XY plane (mm^4)

	Sample 1	Sample 2	Sample 3	Sample 4	Sample 5	Sample 6	Sample 7	Sample 8
1	243.3	280.3	150.6	295.3	252.8	237.8	246.8	117.7
2	171.7	262.0	104.8	205.0	186.5	173.3	165.2	104.4
3	151.3	255.6	97.1	170.6	136.3	133.5	137.6	97.8
4	181.7	256.9	98.0	176.0	122.3	133.4	141.4	98.7
5	477.2	274.9	151.5	237.8	163.9	180.5	168.7	129.3

Appendix C Table 56 – 2nd principal 2nd moment data at 15° in the XY plane (mm^4)

	Sample 1	Sample 2	Sample 3	Sample 4	Sample 5	Sample 6	Sample 7	Sample 8
1	77.6	42.7	40.7	55.5	45.2	55.7	28.2	17.1
2	53.1	40.0	41.9	33.5	28.0	50.3	25.6	18.1
3	68.8	43.3	42.4	34.0	36.3	51.9	29.3	24.3
4	100.9	50.1	54.6	43.4	47.8	53.2	39.3	29.1
5	161.9	60.6	97.5	80.5	109.8	93.6	55.2	42.5

Appendix C Table 57 – Major axis angle data at 15° in the XY plane (deg.)

	Sample 1	Sample 2	Sample 3	Sample 4	Sample 5	Sample 6	Sample 7	Sample 8
1	27.0	18.5	50.7	39.8	41.4	25.9	38.0	33.8
2	12.8	19.1	49.5	39.3	40.7	24.9	39.1	32.7
3	0.2	19.2	58.6	32.5	33.7	31.5	36.9	31.0
4	-18.0	19.0	73.5	25.0	37.6	40.7	40.1	30.1
5	-28.1	19.5	115.0	12.9	27.0	53.2	39.6	22.6

Appendix C Table 58 – Major axis length data at 15° in the XY plane (deg.)

	Sample 1	Sample 2	Sample 3	Sample 4	Sample 5	Sample 6	Sample 7	Sample 8
1	9.7	11.1	8.7	10.8	11.1	10.8	10.6	8.5
2	8.7	10.8	8.2	9.9	10.0	9.2	9.3	8.1
3	8.3	10.6	7.9	9.1	8.5	8.3	8.7	7.5
4	8.3	10.5	7.3	9.0	7.8	7.8	8.5	7.3
5	11.2	10.5	7.1	9.3	7.9	8.1	8.2	7.9

Appendix C Table 59 - Minor axis length data at 15° in the XY plane (mm)

	Sample 1	Sample 2	Sample 3	Sample 4	Sample 5	Sample 6	Sample 7	Sample 8
1	5.2	3.8	4.9	4.6	4.4	4.8	3.3	3.3
2	5.0	3.8	5.2	3.7	4.0	4.8	3.7	3.4
3	5.5	4.0	5.5	3.9	4.4	4.9	3.9	3.8
4	6.1	4.3	4.4	4.4	4.9	4.5	4.4	3.9
5	6.4	4.3	4.1	5.7	6.5	5.4	4.7	4.2

Appendix C Table 60 - Major-to-Minor axis length ratio data at 15° in the XY plane

	Sample 1	Sample 2	Sample 3	Sample 4	Sample 5	Sample 6	Sample 7	Sample 8
1	1.9	3.0	1.8	2.3	2.5	2.2	3.2	2.6
2	1.7	2.8	1.6	2.6	2.5	1.9	2.5	2.4
3	1.5	2.6	1.4	2.3	1.9	1.7	2.3	2.0
4	1.4	2.5	1.7	2.1	1.6	1.7	2.0	1.9
5	1.8	2.4	1.7	1.6	1.2	1.5	1.7	1.9

Appendix C Table 61 - Cross-sectional area data at 20° in the XY plane (mm^2)

	Sample 1	Sample 2	Sample 3	Sample 4	Sample 5	Sample 6	Sample 7	Sample 8
1	41.9	35.8	31.0	40.5	35.7	36.7	32.2	23.7
2	36.0	35.3	29.0	32.7	30.9	34.1	29.1	23.6
3	37.2	35.6	28.6	31.1	30.5	32.0	29.5	24.9
4	42.0	36.5	29.5	33.9	31.4	32.2	31.3	25.4
5	56.2	37.8	35.4	41.8	41.8	40.5	34.8	29.3

Appendix C Table 62 - 1^{st} principal 2^{nd} moment data at 20° in the XY plane (mm^4)

	Sample 1	Sample 2	Sample 3	Sample 4	Sample 5	Sample 6	Sample 7	Sample 8
1	241.1	280.9	155.5	311.6	256.8	231.1	254.8	118.4
2	175.2	266.4	111.6	217.9	197.1	173.5	170.4	106.7
3	158.7	260.4	106.9	180.6	142.2	138.1	149.0	101.4
4	189.0	260.3	107.0	185.5	124.7	138.9	151.3	101.8
5	442.1	267.2	150.3	240.4	166.9	187.1	182.0	127.3

Appendix C Table 63 – 2nd principal 2nd moment data at 20° in the XY plane (mm^4)

	Sample 1	Sample 2	Sample 3	Sample 4	Sample 5	Sample 6	Sample 7	Sample 8
1	87.8	44.4	44.0	60.5	46.6	56.8	29.3	18.2
2	61.8	43.1	45.0	37.8	29.8	56.2	27.9	19.9
3	77.9	45.9	46.6	37.7	38.9	56.2	33.9	26.0
4	108.2	51.0	57.2	49.0	50.2	58.1	43.8	30.4
5	155.3	58.8	96.7	85.0	118.8	98.3	60.7	42.8

Appendix C Table 64 – Major axis angle data at 20° in the XY plane (deg.)

	Sample 1	Sample 2	Sample 3	Sample 4	Sample 5	Sample 6	Sample 7	Sample 8
1	25.5	17.2	51.6	41.3	40.8	24.0	37.6	33.0
2	10.5	17.6	51.3	39.6	39.5	24.3	38.5	31.9
3	-2.2	17.8	59.7	32.5	33.1	32.3	37.2	30.6
4	-22.4	17.8	72.8	25.3	36.8	40.4	41.1	30.0
5	-33.2	18.3	108.1	12.0	29.6	51.4	40.0	23.9

Appendix C Table 65 – Major axis length data at 20° in the XY plane (deg.)

	Sample 1	Sample 2	Sample 3	Sample 4	Sample 5	Sample 6	Sample 7	Sample 8
1	9.5	11.0	9.0	10.8	11.3	10.6	10.6	8.5
2	8.6	10.8	8.4	10.0	10.1	9.1	9.5	8.1
3	8.3	10.6	8.0	9.2	8.6	8.3	8.9	7.6
4	8.4	10.5	7.4	9.0	7.9	7.8	8.6	7.3
5	11.1	10.4	7.0	9.2	7.8	8.2	8.3	7.7

Appendix C Table 66 - Minor axis length data at 20° in the XY plane (mm)

	Sample 1	Sample 2	Sample 3	Sample 4	Sample 5	Sample 6	Sample 7	Sample 8
1	5.5	3.8	5.1	4.8	4.7	4.9	3.4	3.4
2	5.3	3.9	5.4	3.9	4.1	5.0	3.8	3.5
3	5.7	4.1	5.4	4.0	4.5	4.9	4.0	3.9
4	6.2	4.3	4.3	4.6	5.0	4.6	4.5	3.9
5	6.5	4.4	4.0	5.7	6.8	5.5	4.9	4.2

Appendix C Table 67 - Major-to-Minor axis length ratio data at 20° in the XY plane

	Sample 1	Sample 2	Sample 3	Sample 4	Sample 5	Sample 6	Sample 7	Sample 8
1	1.7	2.9	1.8	2.2	2.4	2.1	3.1	2.5
2	1.6	2.8	1.6	2.6	2.5	1.8	2.5	2.3
3	1.5	2.6	1.5	2.3	1.9	1.7	2.2	2.0
4	1.4	2.5	1.7	2.0	1.6	1.7	1.9	1.8
5	1.7	2.4	1.7	1.6	1.1	1.5	1.7	1.8

Bibliography

1. Braden, Bart, “The Surveyor’s Area Formula”, The College of Mathematics Journal, Vol. 17, No. 4. (1986), 326-337

2. Flandry, F, Hommel, G, “Normal Anatomy and Biomechanics of the Knee”, Sports Medicine and Arthroscopy Review, Vol. 19, Issue 2. (2011): 82-92

3. Forsythe, Brian et al., “Dynamic 3-Dimensional Mapping of Isometric Anterior Cruciate Ligament Attachment Sites on the Tibia and Femur: Is Anatomic Also Isometric?”, The Journal of Arthroscopic and Related Surgery, Vol. 34, No. 8 (2018): pp 2466-2475

4. Fu, Feddie H et al., “Editorial Commentary: The Anterior Cruciate Ligament Is a Dynamic Structure”, The Journal of Arthroscopic and Related Surgery, Vol. 34, No. 8 (2018): pp 2476-2477

5. Fujimaki, Yoshimasa et al. “Quantitative In Situ Analysis of the Anterior Cruciate Ligament”. The American Journal of Sports Medicine, Vol. 44, No. 1 (2015): 118-124.

6. Gabriel, Mary T. et al., “Distribution of in situ forces in the anterior cruciate ligament in response to rotary loads”, Journal of Orthopaedic Research, 22 (2004), 85-89

7. Hally, David, “Calculation of the Moments of Polygons”, Defense Research Establishment Atlantic. (1987)

8. Hashemi, J et al., “An alternative method of anthropometry of anterior cruciate ligament through 3-D digital image reconstruction”, Journal of Biomechanics 38 (2005) 551-555

9. Iriuchishima, Takanori et al., “Evaluation of the ACL mid-substance cross-sectional area for reconstructed autograft selection”, Knee Surgery, Sports Traumatology, Arthroscopy, 22 (2014): 207-213

10. Petersen W., Zantop T., “Anatomy of the Anterior Cruciate Ligament with Regard to Its Two Bundles”, Clinical Orthopaedics and Related Research, Number 454 (2007), pp. 35-47

11. Siebold, Rainer et al., “Flat midsubstance of the anterior cruciate ligament with tibial “C” - shaped insertion site”, Knee Surgery, Sports Traumatology, Arthroscopy, 23. (2015): 3136-3142

12. Smith, Lindsay, “A tutorial on Principal Components Analysis”. (2002)

13. Sommer H.J III (2009), polygeom.m, Version 9.0 [MATLAB]

14. Ugural, Ansel C., Fenster, Saul K., Advanced Strength and Applied Elasticity, 4th ed.

15. Zheng L., Harner CD., “The Morphometry of Soft Tissue Insertions on the Tibial Plateau: Data Acquisition and Statistical Shape Analysis”. PLOS ONE, Vol. 9, Issue 5 (2014)